# Strength Failure Mode-based Treatment of S-N curves and Haigh Diagrams for Brittle behaving Materials with emphasis put on Embedded UD Lamina Material

*(a comprehensive collection of the topics in this field with special regard of composite parts)*

Ralf_Cuntze@t-online.de; formerly MAN Technologie AG, Augsburg, Germany,
linked to Carbon Composites e.V. (WG Composite Mechanical Engineering), Augsburg and CC TUDALIT (WG Fiber reinforcement in Civil Engineering), Dresden.
Convenor of VDI 2014 Guideline "*Development of Fibre-Reinforced Plastic Components, Analysis*".

***Keywords:*** *Lifetime prediction, laminates, S-N curve, Haigh diagrams, UD lamina material, fracture failure mode approach*

**Summary:**

Experience shows that multi-directional laminates, composed of endless fiber-reinforced UD laminas, statically designed to a design strain limit of $\varepsilon < 0.3\%$, do not fatigue. However, lightweight design requires a higher exertion of such materials for high-performance applications.

The author presents a rigorous engineering-like method for fatigue life estimation which is equivalent stress-based according to his World-Wide-Failure-Exercise (WWFE)-successful static 'Failure Mode Concept' FMC. This FMC is the main brick of his 'Mises-like' UD strength failure criteria set which is the tool the damaging portions of this brittle behaving material are calculated with.

The proposed method consists of: (1) Novel failure mode-based modeling of the varying operating loads depending stress states; (2) Measurement and mapping of a minimum number of S-N curves which means one basic S-N curve for each activated failure mode namely 2 fiber FF and 3 inter-fiber or matrix fracture failure modes IFF; (3) Novel determination of other necessary S-N curves within a one failure mode by employing Kawai's 'modified fatigue strength ratio' together with the obtained basic S-N curve of this failure mode; (4) generation of failure mode-linked FF and IFF Haigh diagrams which involve all S-N curves necessary for fatigue life estimation; (5) Novel design-desired Constant-Fatigue-Life (CFL) curves, directly and automatically computed by the presented method; (6) Application of Miner's rule for the embedded lamina in order to accumulate the FMC-computed damaging portions.

The method will enable an effective and faster design development after the transfer from the embedded lamina to a general laminate will be validated by further investigations. Tests for embedded laminas together with multi-layered multi-directional laminate test specimens are required to capture the occurring in-situ effect.

The performed work has been still applied in a research project to design energy storage rotors (wheels). These are composed by modular systems of different output classes, such as the Stornetic EnWheel: 188 kWh up to 188 kWh per day.

# 1 Introduction

## *1.1 Design Aspects*

*System and concurrent engineering of the involved technical disciplines analysis and simulation are recognized as key enablers to increase competitiveness.* The thereby applied tools must give confidence to the designer [Cun16d].

Composite components with very different matrices are used in primary load carrying structures in Aircraft, Automotive, Mechanical and Civil Engineering. These composites are composed of Fiber Reinforced Polymer or Concrete or other matrix materials), taking advantage of the increased structural strength and stiffness to weight ratios, of corrosion resistance, or of more innovative design capabilities.

Increasing use requires a better understanding of the composite's behavior under static, cyclic, and impact loading while being exposed to various environments. *Fig.1* presents a look at the structural Design Verifications to be provided in order to obtain Structural Integrity as precondition for product certification by a load Reserve Factor $RF > 1$. Such a design may consider thick composite sections with large numbers of layers, regions of significant ply drop off, sandwich constructions and bonded joints, eventually also braided materials may be used. Therefore, design verification is pretty difficult to perform and can often only be partly reliably solved by incorporating expensive structural tests.

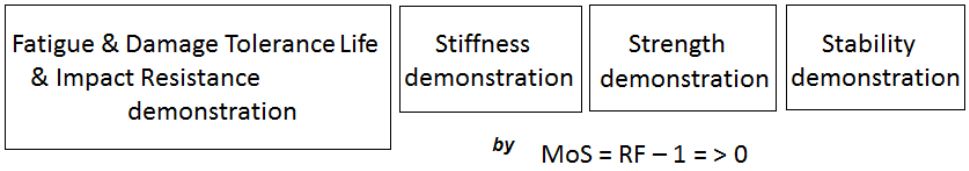


*Fig.1: Necessary Design Verifications. Margin of Safety MoS, Load Reserve Factor RF*

Modern light-weight structures are the result of an optimization compromise between all the product's functional requirements such as stiffness and strength, and of the operational requirements such as lifetime. Design driving are – beside the *actions* (loadings) – all the *resistance* affecting quantities - the material properties and the failure conditions for initiation of failure and also for final fracture of the usually relatively brittle behaving composite materials. The material addressed here is the transversely-isotropic UD lamina.

Responsible for the goodness of the structure, designed under e.g. a minimum mass requirement, are a qualified analysis procedure, an input of reliable design data involving the material properties, including dimensioning load cases and the safety concept. Special task of the designer is the development of a so-called robust structure that does not essentially change its behavior under the usual scatter of all the stochastic design parameters. When doing this the engineer must rely – regarding the designed product - on the existence of qualified processes such as validated software, analysis, tests and manufacturing as well as NDI procedures. And all this must be considered the more under cyclic loading.

Failure is defined as: *The structural part does not fulfil its functional requirements*. Here, typical failure modes are the strength failure modes fiber failure FF and inter-fiber-failure IFF, also termed matrix failure, leakage of a composite vessel, a deformation limit of a composite rotor or a delamination size limit within a laminate. Traditionally, First-Ply-Failure FPF (nowadays often seen as onset of damaging or of failure) and Last-Ply-Failure LPF (final fracture, usually sudden fracture occurs after last FF) are distinguished. Failure may be also a distinct damaging sum $D_{admissible}$ as the result *of the accumulation of damaging portions under cyclic loadings.*

Failure Assessment is mandatory and must include structure, laminate and lamina (ply). Thereby, it is to discriminate between tolerable failure and final fracture failure which might be a catastrophic one.
*Note: What failure is, must be always defined - for each application - as a project-depending task for obtaining the right design.*

For UD materials 5 failure modes must be taken into account together with their degradation effects: FF1 (tension) and FF2 (compression, *kinking*), Inter-Fiber-Failure IFF1 (tension), IFF2 (compression) and IFF3 (in-plane shear). First-Ply-Failure which includes onset of delamination of a ply in thickness direction can be predicted by 3D UD strength criteria [Cun04, 13, 14, Puc02, Chr13], (SFC, strength failure condition is the correct term, we write $F = 1$).
Of course, FF means final catastrophic failure. Dependent on the laminate in the structural part the same may be valid for IFF2, whereas IFFI (lateral tension, Puck mode A) and IFF3 (shear) behave more benign and residual strength and stiffness capacity are not suddenly lost after FPF, but they continuously decay with increasing degradation.
The grade of the criticality of a distinct failure needs to be assessed in each project application due to the active softening curve of the embedded ply. Under monotonic loading at first diffuse and later discrete (localized) micro-damaging takes place. Under cyclic loading damaging is more diffuse than under increasing monotonic static loading.

Brittle behaving UD materials exhibit 5 fracture failure modes which means the measurement of 5 basic S-N curves as observation proves and material symmetry requires. Of course, failure modes interact and this is considered by an interaction formula (for more details, see *Annex*). According to the basic stress states there exist 3 Haigh diagrams for FF1 (fiber tension) with FF2 (fiber compression), IFF1 (lateral tension) with IFF2 (lateral compression), and eventually for IFF3 (in-plane shear). The author will present later these constant-fatigue-life (CFL) diagrams.
There are many effects causing non-linearity such as large deformations (geometry), large strains (inelastic material), change of fiber orientation (in-plane fiber waviness and waviness between layers), and post-initial failure behavior due to degradation which requires the consideration of the softening $\sigma$-$\varepsilon$ curve part (*Fig.2*). Non-linearity significantly determines the cyclic damaging process.
In compression domain usually inelasticity (ductility) is given, dependent on the multi-axial compression level), However, for porous materials (very small Poisson ratios) under compression ductility practically does not exist, see [Cun16].

### *1.2 Objectives*

In static design of non-ductile behaving materials the basic input is the number of the material strength values. Observation documents: *Each single static strength governs just one single strength failure mode.* In cyclic design, a project task-dependent number of S-N curves must be provided. The presented Haigh diagrams involve all these S-N curves necessary for fatigue life estimation of variable amplitude loading. Experience proved that the static Strength Failure Conditions SFCs are also applicable for the determination of the damaging portions as long as the failure behavior remains the same under cyclical loading, too.

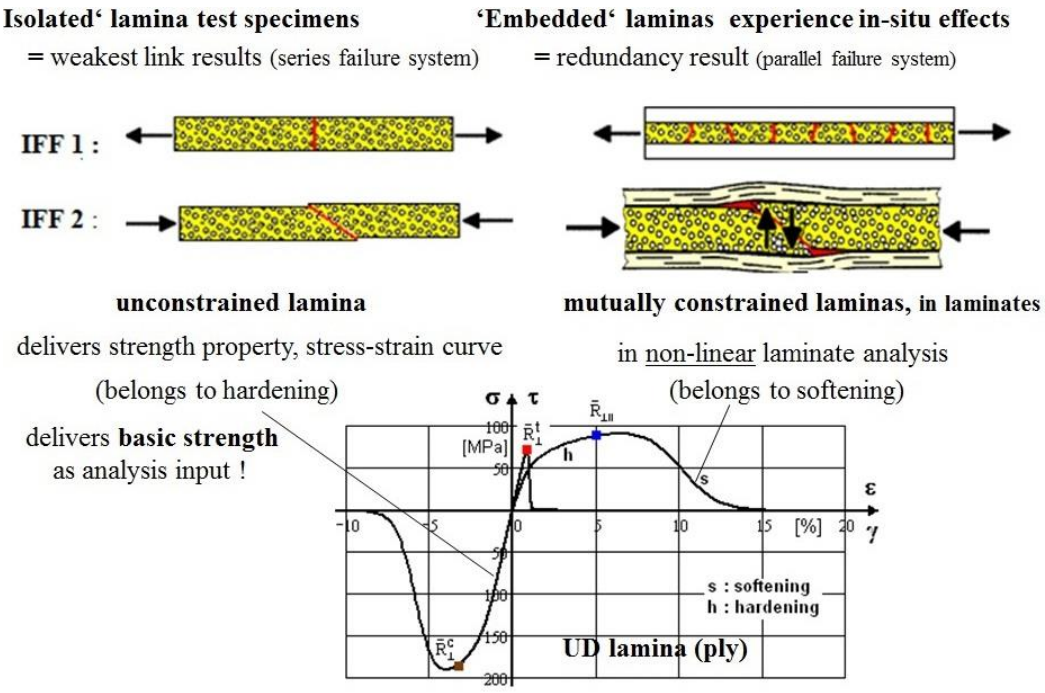


*Fig.2: UD material test specimen. Isolated (generates hardening curve) and embedded (causes a softening curve part)*

The following approach focusses several objectives:

*First*: Since the measurement of S-N curves is very costly it is of highest interest to reduce the test program to a minimum one. The idea is to achieve this by measuring just one basic S-N curve for each strength failure mode and to theoretically predict other S-N curves necessary for non-constant amplitude lifetime predictions on basis of this basic curve and the application of a suitable supporting model.

*Second:* An attempt to automatically calculate the required constant life curves of the Haigh diagram, because interpolation in Haigh diagrams are an effortful task for a reliably designing engineer and should be automatically performed.

*Third:* A strength failure mode approach considering the embedded (not the isolated) lamina and not the laminate anymore. *Fig.2* displays the differences between so-called isolated and embedded laminas (plies). This approach should lead to a generalization with the consequence that for designing with a new laminate a test series would be not necessary. Such a novel way is according to an agreement within the German academic BeNa (Betriebsfestigkeits-Nachweis) group, founded by the author in 2010. The members of this group agreed to establish fatigue-life models not on basis of laminates but on the embedded lamina to enable an effective and faster design development when the transfer from the embedded lamina to a general laminate will be validated in future. Doing this, special fatigue tests for embedded lamina test specimens together with multi-layered multi-directional laminates are required.

Of highest concern in a Haigh Diagram is the course of constant fatigue life curves in the transition zone between the mode-dominated domains at the left (negative mean stress, $\infty > R > 1$) and the right (positive, $1 > R > 0$). In the center, the CFL curve part is the damaging result of two commonly activated modes. The stress ratio R = - 1 delivers some validating test points in the transition zone where crack-closure effects occur. More representative for this regime is $R_{trans}$ = compressive strength / tensile strength and should be tested.

How S-N curves are mapped by mathematical functions is depicted in the over-next chapter. For $n > 10^4$ the S-N curves of notched and ‘plain’ composites narrow.

In this paper the classical fatigue task *'damaging* (Schädigung) *of a non-cracked material'* is investigated. A technical damage (Schaden) such as a delamination crack in composite structures, caused due to the accumulation of damaging portions or caused by an impact are not treated here. A damage tolerance concept with its fracture mechanics tools must be applied then.

### 1.3 Fatigue and Damage Tolerance

#### *Fatigue*

Cyclic failure behavior of fiber reinforced plastic (FRP) composites is quite different from that of a ductile behaving metallic material. A general engineering-like method for the estimation of the life-time of high-performance UD-lamina material-based laminates does not yet exist [Koc16, Cun10]. A reliable method is highly desired, generally applicable to different laminas and laminates.

Essential for the lifetime analysis is the stress level: Low Cycle Fatigue LCF means high stressing, High Cycle Fatigue HCF means intermediate stressing and Very High cycle Fatigue VHCF low stressing and straining (for instance with wind energy rotors, helicopter blades). Whether the damaging driver remains the same from LCF (e.g. the EnWheel) until VHCF must be verified in each given case. The induced stress level at which fatigue failure occurs is lower than that for static loading. Initiation of fatigue failure in composites is firstly diffuse and later discrete (localized) micro-damaging takes place at distinct material locations. It is affected by the environment such as by hygro-thermal effects in the case of polymer-matrix composites, i.e. Carbon Fiber Reinforced (CFRP) or Glass Fiber Reinforced Plastics (GFRP). For these types of composites experience proved, that if different fiber orientations given in the UD lamina-composed, multi-directional endless fiber-dominated laminate then a fatigue design verification is not necessary, presumed, a static 'fiber-dominated design' is performed for a limit design strain of $\varepsilon < 0.3\%$ . However, future lightweight design requires a higher exertion of this material. CFRP Laminates may show an endurance limit. For fiber-dominated designed laminates the representative mode is fiber failure, the mode FF1, activated under the variable tensile stresses.

Cyclic loadings are most often given by an operational loading spectrum which means a loss of the stress-time relationship.

For above composites, usually the same procedure is applied as for the more or less ductile behaving metals. However, physically much better fits a dedication to brittle behaving metals since these are more related - not looking at anisotropy - to the usually brittle behaving composite materials. They also experience two different fracture failure modes under tension (normal fracture NF) and under compression (shear fracture SF or crushing fracture CrF).

Ductile behaving metals underlay the same single yielding failure mode under tension and under compression, whereby the so-called mean-stress effect is much smaller than in the brittle case.

#### *Damage Tolerance*

*Damage Tolerance* (not addressed further) is a property of a structure related to its ability to safely sustain a damage until its repair or replacement can be affected. It builds upon the determination of damage growth and the establishment of inspection plans. It uses fracture mechanics to describe delamination crack growth under operational cyclic loading. A maintenance program must detect the damage and initiate the repair of accumulated and sudden accidental damage, applying 'reject and accept criteria' for quality assurance. Fatigue

consists of life until onset of damaging (*objective of the paper*) and further growth until damage initiation.
Questions an engineer poses in the case of cyclic design: When does damaging start? How can one consider the single micro-damaging portion (= Schädigung)? How can the single damaging portions be accumulated essential for *fatigue verification*? When do the accumulated damaging portions form a damage ? When does such a damage (= Schaden, usually a delamination) become so big to be of a critical size ? How is the damage growth (task for *damage tolerance verification*) in the final phase of fatigue life in order to determine a part replacement time or the inspection intervals ?

## 2 Structural Modeling of Laminated Parts and Design Aspects

There are several possibilities to model a laminate. The first is to homogenize the constituents matrix and fiber to a transversely-isotropic lamina material. A second is to use laminate properties and a third to stay on the microscopic level of the constituents and bridge by meso-models to the lamina macroscopic level.

*Fatigue Design Analysis and Design Verification* are performed on the levels (1) *Structure*: forces and moments (e.g. pressure load of a tank); (2) *Cross-section*: section forces and section moments (beams, shell wall), and (3) *Material:* stresses in a material 'point' within the structure. In the last case the first task is to transfer the loadings into stress states considering proportional and non-proportional stresses. In the LCF regime non-linearity causing effects such as creeping, relaxation are met.

The structure's load-carrying capacity is mainly *locally* determined: In the critical material locations of undisturbed areas or plain areas respectively by the local stress state; in disturbed areas like holes or at stress-raising stiffness jumps by a stress concentration (notch mechanics to employ); and at delamination sites within a laminate by stress intensity which affords the application of fracture mechanics. These stress situations are related to different strength quantities better termed resistances such as the classical strength $R_{\perp}$, the notch strength, and the fracture toughness *G*. Here, stress and material strength are addressed.

Generally, design analysis means investigation of the average behavior of the structural component. Therefore, average (typical) physical properties, including an average stress-strain curve with average strength values, are applied whereas in design verification of the chosen design statistically-based minimum and maximum properties are utilized. The use of average values predicts a structural behavior that meets the real behavior best, namely with a 50% expectance value. This is also valid when validating fatigue models.
At present, usually a semi-probabilistic safety concept is applied in mechanical engineering for design verification: It employs: (1) a factor of safety *j* to increase the actions or respectively the external loadings (e.g. $j\cdot$ Design Limit Load = $j\cdot DLL$ = Design Load *DL*) and (2) takes statistically minimum values for the resistances (strength etc.) in order to further implement reliability into the structure.
Adequate UD strength failure conditions SFCs are necessary to compute the damaging portions: For UD-materials the World-Wide-Failure-Exercises-I and -II have tested all available strength conditions and sorted out the better ones. Cuntze's 3D Failure-Mode-Concept (the 'Mises' under the UD 'criteria') and Puck's 3D Action Plane-Criteria could map the provided accurate test data best. About 30% of the WWFE data sets were not correct. Above 3D strength conditions are also capable of predicting onset-of failure in thickness direction. However, then lower strength values are used in thickness direction than in the lamina plane in order to simpler strength-verify the orthotropic material effect in thickness on

top of the transversely-isotropic lamina material model and analysis. Engineering practice desires macro-mechanical SFCs but – as failure occurs at the constituent level - these SFCs must reflect constituents' failures, such as considered in Cuntze's SFCs, see *Annex* and [Cun12].

## 3 Mapping of Fatigue Test Data to Obtain an appropriate S-N Curve

### *3.1 General*

Fatigue failure may occur if the structural material is cyclically loaded. Cyclic loadings are most often given by an operational loading spectrum with its loss of the stress-time relationship. For the design, S-N curves are to formulate. There are two possibilities to present them: (1) using the stress amplitude $\sigma_a(N)$, also termed alternating stress, and (2) using the maximum or upper stress $\sigma_{max}(N)$, usually termed *fatigue strength*. In the case of brittle behaving materials the latter is physically simpler to understand and the stress man is more familiar with this since the decaying curve is interpretable as decaying 'static' strength after a damaging process with *n* cycles. The interesting relationships in fatigue read:

$$\sigma_{\max} = \Delta\sigma/(1-\mathrm{R}) \equiv [2\cdot\sigma_a/(1-\mathrm{R})] \quad \text{with} \quad \Delta\sigma = \text{stress range}\ , \tag{1}$$

$$\mathrm{R} = (\sigma_m - \sigma_a)/(\sigma_m + \sigma_a),\ \ \sigma_a = 0.5\cdot\sigma_{max}\cdot(1\text{-R}),\ \sigma_m = 0.5\cdot\sigma_{max}\cdot(1+\mathrm{R})\ . \tag{2}$$

Hence, in the case of brittle behaving materials the strength value $R_m = R^t = \sigma_{\max}$ ($n = N = 1$) is preferably used as origin and anchor point of the curve, see *Fig.3*.

*<u>Note</u> on some notions for brittle behaving materials: (a)* R = 0, *termed tensile pulsating or fluctuating (swelling) stress, activates just the fracture failure mode Normal Fracture NF if n* = 1 = 2·$N_f$; *(b)* R = - 1 *means fully reversed alternating stress, that activates two modes, NF and Shear Fracture SF under compression.* $N_f$ *means half cycle. Practically, the materials stressing effort Eff = 100% changes for N > 1 to the sum of accumulated damaging portions D = 100%.*

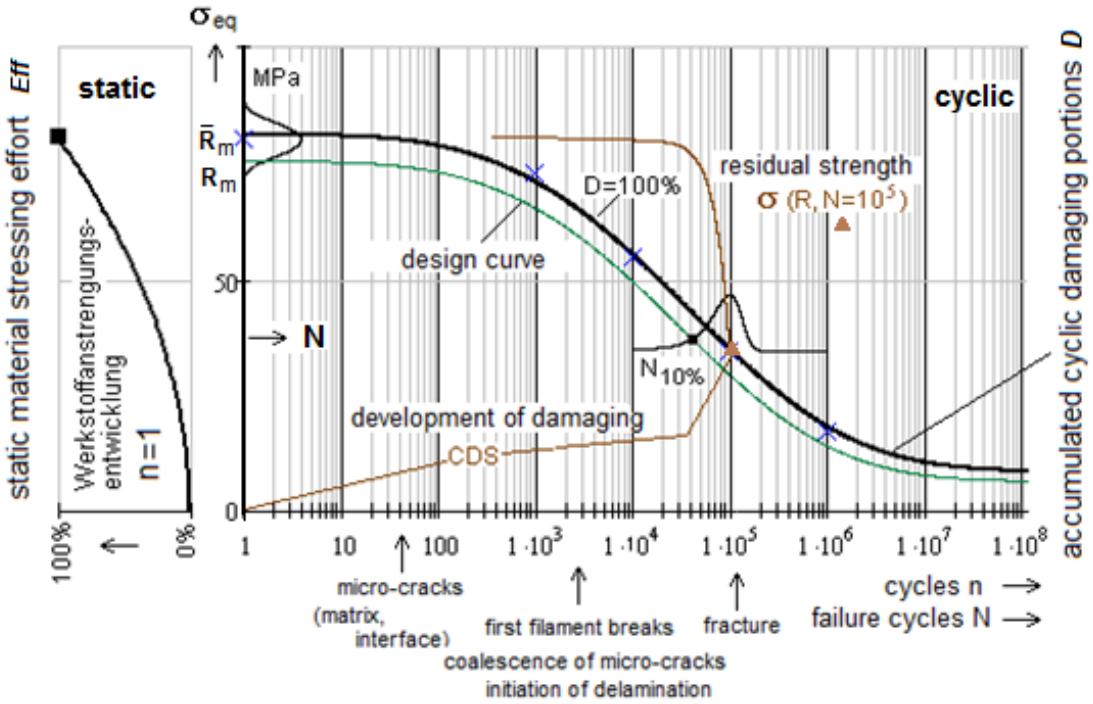


*Fig. 3: Lin-log plotted S/N curve for a distinct stress ratio* $\mathrm{R} = \sigma_{\min}/\sigma_{\max} = 0$ *with development of damaging for a distinct fracture cycle number* $N = 10^5$, *CDS = characteristic damaging state; Eff = material stressing effort ("Werkstoff-Anstrengung") ≡ D (N =1),* $\bar{R}_m$ *= average ultimate strength,* $R_m$ *= ultimate strength design allowable*

### *3.2 Comparison, Choice and Application of a Appropriate S-N curve Models*

Possible mapping formulations are non-linear curves such as given by the Weibull-model and the Wearout-model, [VDI 2014], or linear models in the log-log diagram. Below, five S-N curve mapping models are investigated and displayed in *Fig.4.* As still mentioned, for brittle behaving materials it is physically reasonable to use the strength (average value, bar over) or failure stress $\sigma_{max}$ at $n = N = 1$ as one anchor point in each failure domain $1< R< \infty$, $0< R <1$ (is not valid for R = -1, due to two modes are acting). This reduces the number of free parameters by one. The choice of the S-N model mainly depends on the fact whether an endurance limit for VHCF is given, that should be mapped or not. Such an endurance limit should exist for FF1 of CFRP.

***(1) 3 free parameter-Weibull + strength point***

This model goes through the strength point and maps the endurance limit.

$$\sigma_{\max}(N) = c1 + \frac{\bar{R} - c1}{e^{\left(\frac{\log(N)}{c3}\right)^{c2}}}$$

***(2) 2 free parameter-Weibull + strength point***

This model fits similar well the endurance limit in the HCF domain, like the (1) model.

$$\sigma_{\max}(N) = \frac{\bar{R}}{e^{\left(\frac{\log(N)}{c3}\right)^{c2}}}$$

***(3) Sendecky's Wear-out Model: 2 free parameter + strength point***

$$\sigma_{\max}(N) = \bar{R} \cdot \left(\frac{1 - c1}{N - c1}\right)^{c2}$$

***(4) 2 free parameter + strength point***

$$\sigma_{\max}(N) = c1 \cdot \bar{R} \cdot N^{c2}$$

***(5) 1 free parameter + strength point***

$$\sigma_{\max}(N) = \bar{R} \cdot N^{c1}$$

is straight line in *log-log* diagram $\log \sigma_{\max}(N) = \log \bar{R} + c1 \cdot \log N$ .

In *Fig.4*, the five mapping results - exemplarily for FF1 test data of a CFRP material - are collected

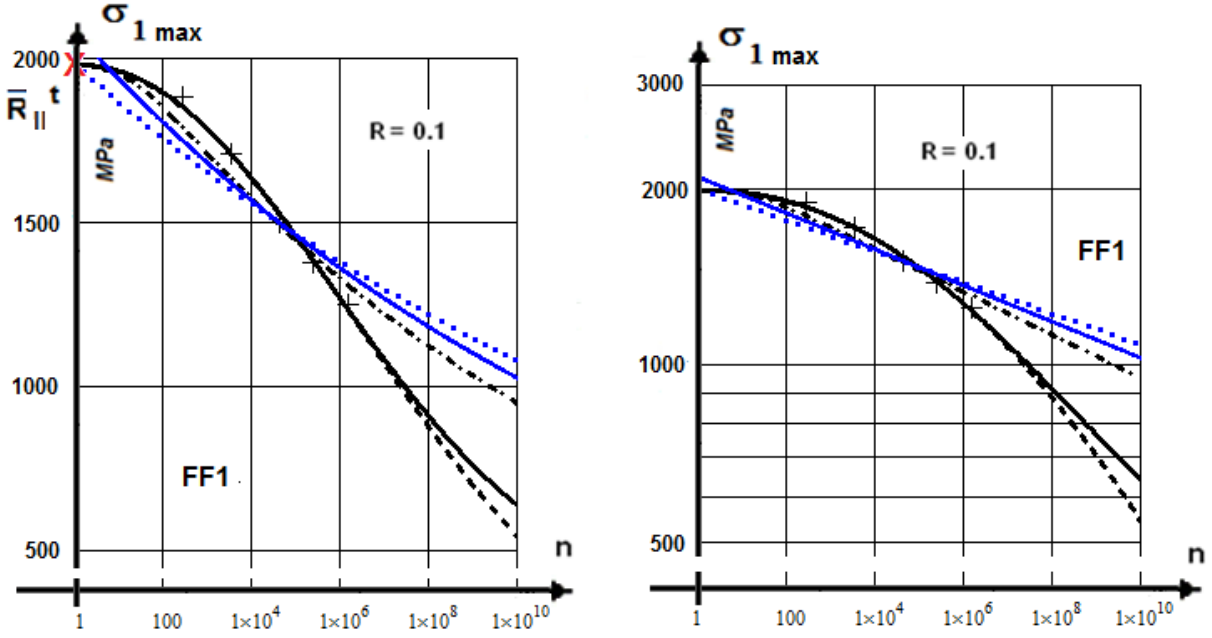


*Fig. 4: Comparison of S-N data mapping capabilities of various curve models in a lin-log and a log-log diagram (test data: courtesy Kawai)* $\bar{R}_{\parallel} \backsimeq$ 1980 MPa

. The following conclusions can be drawn considering the desire "use of a minimum number of free parameters", just so much as physically necessary in the given case.
In the HCF-regime, $10^3$ through $2 \cdot 10^6$, the course of test data can be mapped as follows:

- Lin-log curves: model 1 and 2 work very well. Model 2 approximately considers an endurance limit in the VHCF regime
- Log-log curves: models 1, 2 show highest mapping capability due to the higher number of free parameters. The simple model 5 may work sufficiently well for appropriate courses of test data.

*Fig.5* displays as example the mapping of a small sample size of FF1 test data with model 5. Since the test data set is for the stress ratio R = 0.1 (the measurement of R = 0 is instability jeopardized) it represents the basic FF1 S-N curve with R = *stress ratio*, $\overline{R}$ = *average strength.* Considering the stochastic nature of the problem, it often seems to be sufficient for engineering application to apply the S-N curve mapping model 5.

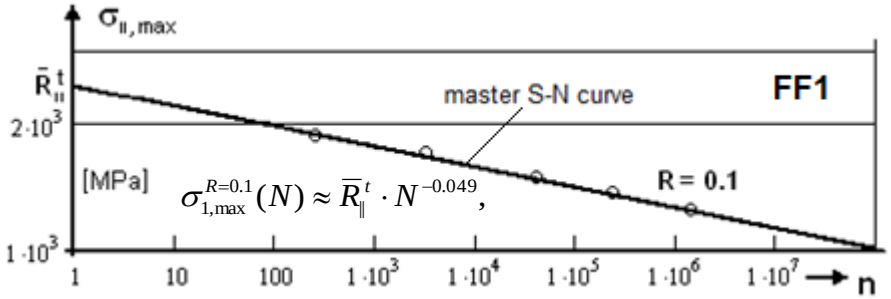


*Fig.5: Mapping of the mode-representative Basic S-N curve [test data: Kawai]*

A Fatigue-life-model (there are also other models stressed) that applies S/N curves needs many test data. In order to reduce the tremendous test effort, it would be very effective to perform a lifetime prediction for a laminate on basis of an *in-situ basic lamina S/N curve* for each single failure mode. Further S/N curves for the same failure mode, required in variable amplitude fatigue analysis, can be predicted from the basic S-N curve by utilizing Kawai's 'modified fatigue strength ratio' model [Kaw04]. This combined procedure enables the engineer during pre-dimensioning to perform lifetime estimations (predictions) for variable loading much quicker.
*Notes: (1) Well-designed CFRP laminates show flat S-N curves which results in a wider scatter. (2) For N > $10^4$ the S-N curves of notched and 'plain' composites narrow. (3) There is some hope that at least for fiber-dominated laminates an embedded (in-situ) lamina fatigue design may replace the laminate design.*

How the determination of other mode-linked S-N curves works? This will be depicted now.

## 4 Determination of other S-N curves on Basis of Basic S-N Curve and Employment of an Appropriate Model, *Example FF*

### *4.1 Application of Kawai's 'Modified Fatigue Strength Ratio'*

*Assumption: The 'Modified Fatigue Strength Ratio' is prediction-capable*
The application of his model is as follows. Kawai first normalizes the fatigue strength $\sigma_{max}$ by the static strength $R_{||}{}^t$, which means the use of the (static) *material stressing effort* (bar over *R* skipped here, due to simpler writing)

$$Eff^{||\sigma} = \sigma_{max} / R_{||}{}^t .$$

*Eff* corresponds to Kawai's $\psi$, termed *'fatigue strength ratio'*. Using the amplitude $\sigma_a$ and the mean stress $\sigma_m$, then the static failure condition above can be expressed as

$$Eff^{||\sigma} = (\sigma_a + \sigma_m)/ R_{||}^{\,t} \equiv \psi. \qquad . \qquad (3)$$

In the fracture case, meaning $\psi = 1 = 100\% \equiv Eff^{||\sigma}$, this reads for the stress case tension

$$\psi = 1 = \sigma_{max}/ R_{||}^{\,t} = (\sigma_a + \sigma_m)/ R_{||}^{\,t} \quad or \quad 1 = \sigma_a / ( R_{||}^{\,t} - \sigma_m ),$$
$$where\text{-}in \quad \sigma_a = 0.5\cdot\sigma_{max}\cdot(1- R),\ \sigma_m = 0.5\cdot\sigma_{max}\cdot(1+R).$$

Analogically to $\psi$, Kawai defines the also non-dimensional '*modified fatigue strength ratio*'

$$\underline{\sigma > 0}: \quad \Psi_t = \sigma_a / ( R_{||}^{\,t} - \sigma_m ) = 0.5\cdot(1- R)\cdot \sigma_{max} / [ R_{||}^{\,t} -0.5\cdot(\mathbf{1}+R)\cdot \sigma_{max}] \text{ or} \qquad (4)$$
$$= 0.5\cdot(1-R)\cdot Eff^{||\sigma} / [1 -0.5\cdot(1+R)\cdot Eff^{||\sigma}] \quad \text{with } \sigma_{max} > \sigma_{min}$$
$$\underline{\sigma < 0}: \quad \Psi_c = \sigma_a / ( R_{||}^{\,c} - \sigma_m ) = 0.5\cdot(1-R)\cdot \sigma_{min} / [ R_{||}^{\,c} -0.5\cdot(1+R)\cdot \sigma_{min}] \quad \text{with } |\sigma_{min}| > |\sigma_{max}|,$$

(corresponding to a *cyclic material stressing effort*) as a scalar quantity and thereby he could introduce the stress ratio *R*. According to being a material quantity $\Psi$ is positive.
Fitting the course of test data, Kawai obtains a Master $\Psi$-curve. Based on the chosen mapping function for $\sigma_{max}$ the FF-linked S-N curves can be estimated by the resolved equations

$$\sigma_{max}(R) = (2\cdot R_{||}^{\,t}\cdot \Psi_{master}) / [\Psi_{master} - R + R\cdot\Psi_{master} + 1], . \qquad (5)$$
$$\sigma_{min}(R) = (2\cdot R_{||}^{\,c}\cdot \Psi_{master}) / [\Psi_{master} - R + R\cdot\Psi_{master} + 1],$$

The application looks promising and this model will be used later for the determination of other S-N curves within a mode.

*Table 2* includes all formulas needed to understand and to determine the requested S-N curves from the basic S-N curve. The example is fiber failure FF.

*Table 2: Formulas to map the basic S-N curves $\sigma_{max}$ (R>0) , $\sigma_{min}$ (R<∞) and to determine Kawai's Master $\Psi$-model, example FF*

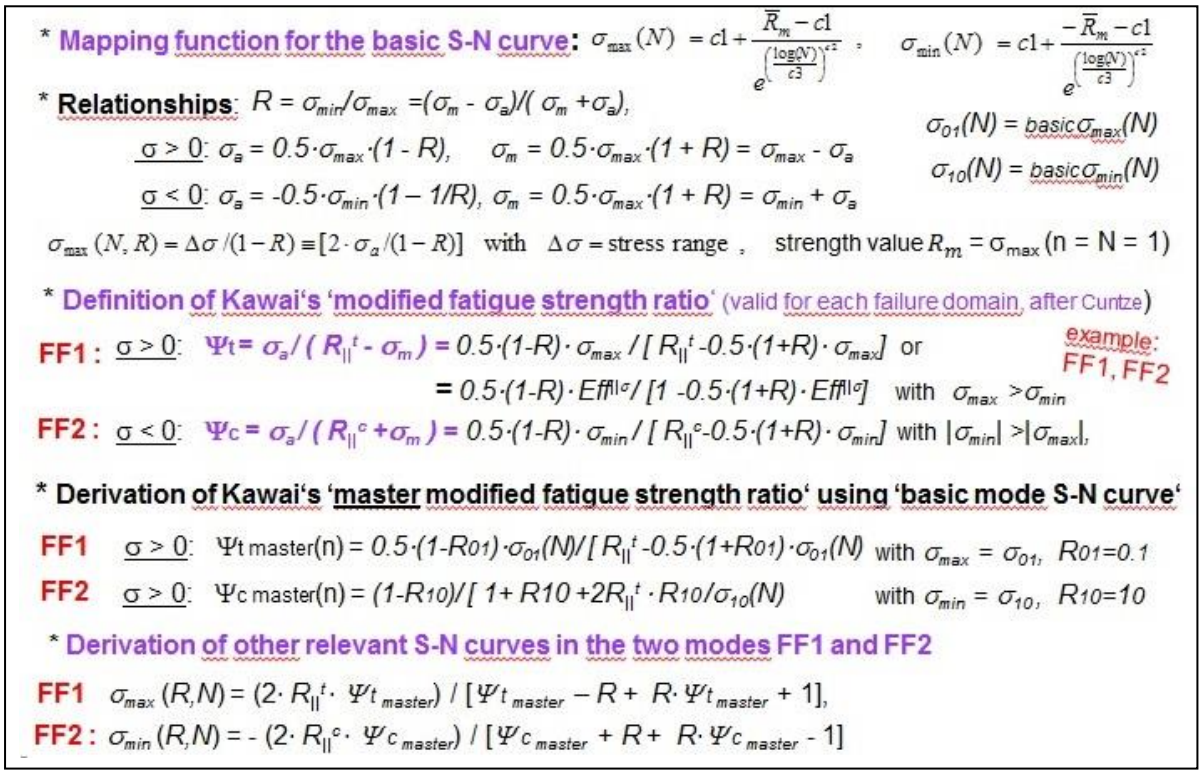


*However mind: Cuntze dedicates a Master $\Psi$ curve to each single failure mode NF or SF in contrast to Kawai who normalizes the test data of all R-curves to a band of scattering test points which he then maps by one single Master $\Psi$ curve.*

For deeper explanation *Fig.6* presents for the 5 UD failure modes some associated characteristic uni-axial S-N curves.

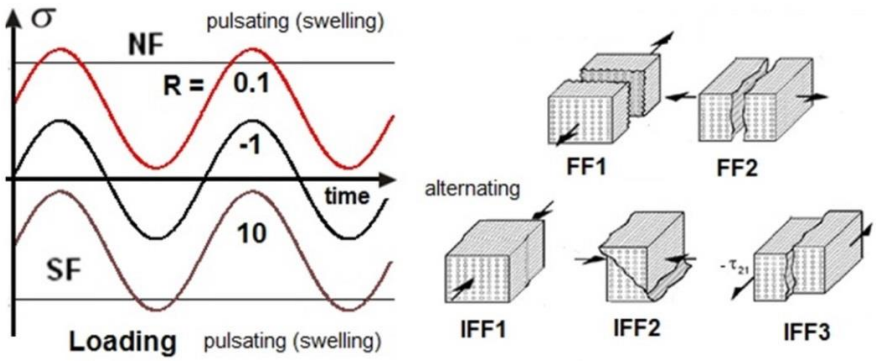


*Fig. 6: Characteristic uni-axial S-N curves and the 5 UD failure modes*

Then *Table 3* provides the full procedure by presenting all steps and a visualization, using a simple linear S-N curve mapping model 5 $\sigma_{max}(N,R) = \bar{R} \cdot N^{c1}$ .

*Table 3: Steps to predict other FF1 S-N curves from the basic S-N curve and Kawai's model*

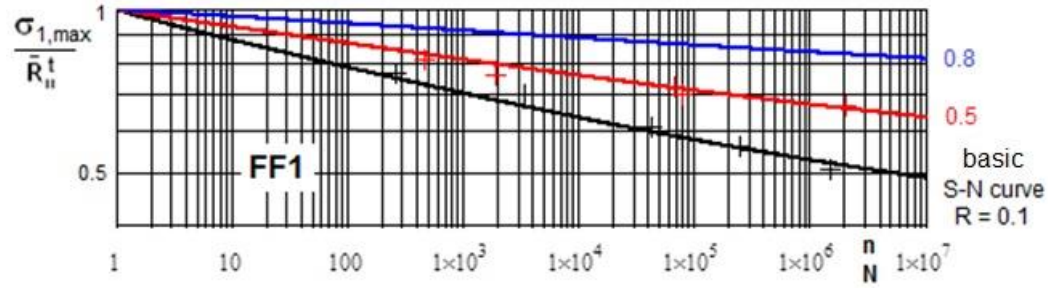


1. Establishment of the Basic mode S-N curve from test data
2. Further necessary S-N curves might be measured or estimated by a suitable model. Chosen here is Kawai's "modified fatigue strength model Ψ"
3. Calibrating of the Master Ψ model curve by the measured Basic mode S-N curve test data
4. Estimation of other S-N curves on basis of 'basic mode S-N curve + Kawai's Master Ψ model curve'

*Fig.7* eventually compares *Ψ* model-predicted IFF S-N curves and the two mode-linked basic S-N curves. Some available test data are displayed.

*Lessons Learned from these mode-linked applications (the associate basic IFF S-N curves are* R = 0.1, 10*): The Ψ-model captures the extreme S-N curves* R = 0, 1 *(NF),* 1000, 1 *(SF), but predicts intermediate curves such as* R = 0.5 *too much on the conservative side. The Ψ model can be tuned to capture this better.*

### *4.2 Fracture Failure Mode-related Discussion of Haigh Diagrams*

A concentrated display of S-N curves is performed by Haigh diagrams $\sigma_a(\sigma_m)$, using the amplitude as ordinate and the mean stress as abscissa, see *Fig.8*. Over the mean stress range of for instance an isotropic material, $-R_c$ through $R_t$, the stress ratio R spans from 1 via 10 to $\pm\infty$ and via -1 to 1. To demonstrate the failure mode-linked view of the Haigh diagram, in *Fig.8* the simpler understandable isotropic case is displayed with its two fracture failure

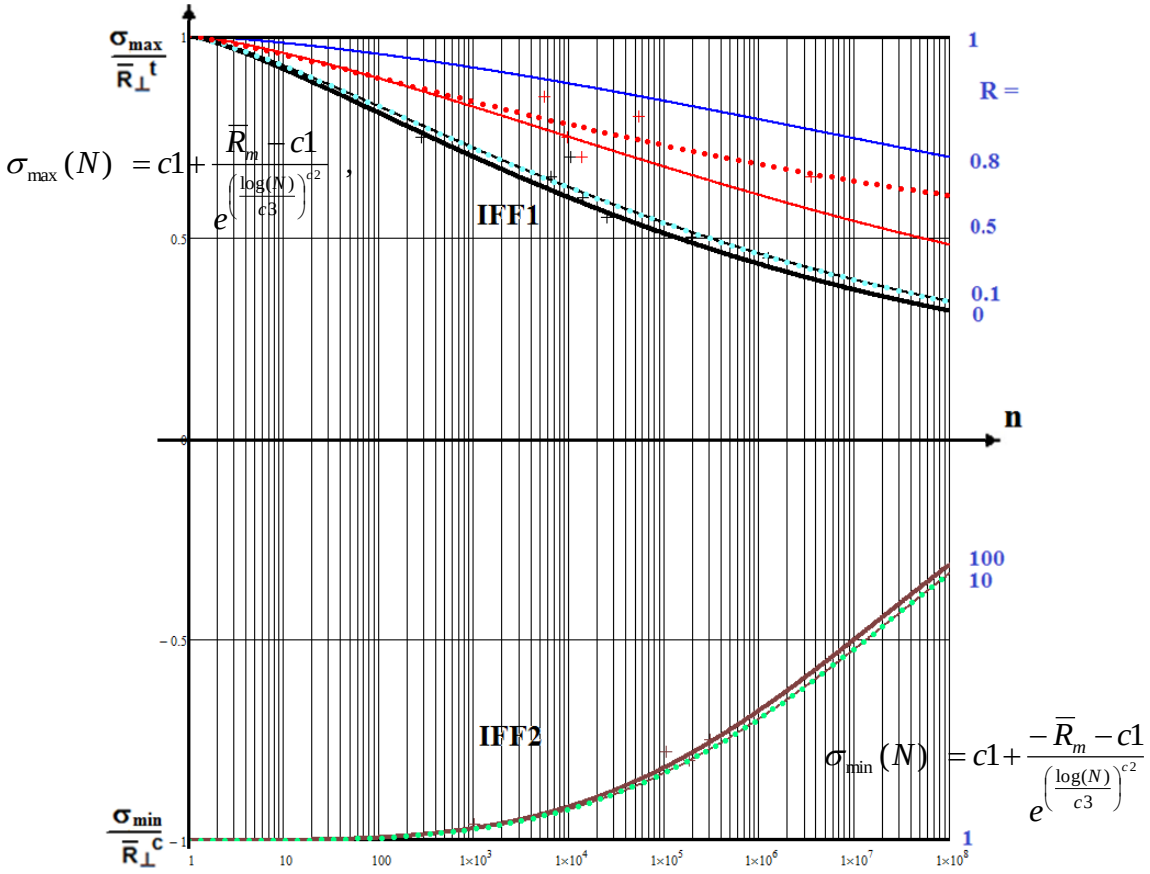


*Fig.7: Comparison of Ψ model-predicted IFF S-N curves (bold) and the 2 Basic mode S-N curves (R = 10, 0.1) from mapping with model 1 (dotted, not tuned) with some test data*

modes Normal Fracture NF under tension and Shear Fracture SF under compression. There are two failure mode domains and a transition zone in between the two modes where mode interaction takes place. The outer straight lines of the figure display the static curves as boundary curves. This is not identical to the constant fatigue life CFL curve $N$ =1. Further, the course of the stress ratio $R(\sigma_a, \sigma_m)$ is shown.

The two failure domains are marked by the associated $R$-domains: SF with $1 < R < \infty$ and NF with $1 > R > 0$. Of further interest is $R_{trans}$ which practically separates in the transition zone both the failure domains from another. This stress ratio is the most 'transition neutral' one.

In the transition zone, the CFL curve is the damaging result of two commonly active modes or in other words a joint action of the two modes NF and SF. The fully reversed stress, stress ratio lies more or less central (central only if $R^c \approx R^t$) in the transition zone with two parts separated by the stress ratio line $-R^c/R^t$. Hence, R = -1 'only' delivers test points in the transition zone which may be often not optimally located. Consequently, one should better measure the not well termed critical stress ratio ([VDI2014]. Due to the fact that $R_{cr} = -R^c/R^t$ has nothing to do with criticality the author renamed $R_{cr}$ in $R_{trans}$. This $R_{trans}$ is more generic for the transition zone than R = - 1, being just a special case of $R_{trans}$ if both the strengths are of equal size. At $R_{trans}$, maximum interaction takes place. In the transition zone micro-crack-closure effects occur.

*Notes drawn from Figs. 7, 8: (1) Cuntze describes Haigh diagrams failure mode-wise. (2) The N = 1 constant fatigue life curve is not identical to the straight static envelopes, because two failure modes are acting in the transition zone.(3)* $R_{trans}$ *represents the test data situation in the transition domain better than* R = -1. *(4) Obvious is that for brittle behaving materials clear sectors are given for the dominating fracture failure modes. (5) The mode boundary S-N*

*curves* R = 0 *and* ∞ *can be calculated by using Kawai's approach. Hence, they deliver the anchor points for the 'linear' CFL functions in the pure mode domains of the Haigh Diagram.*

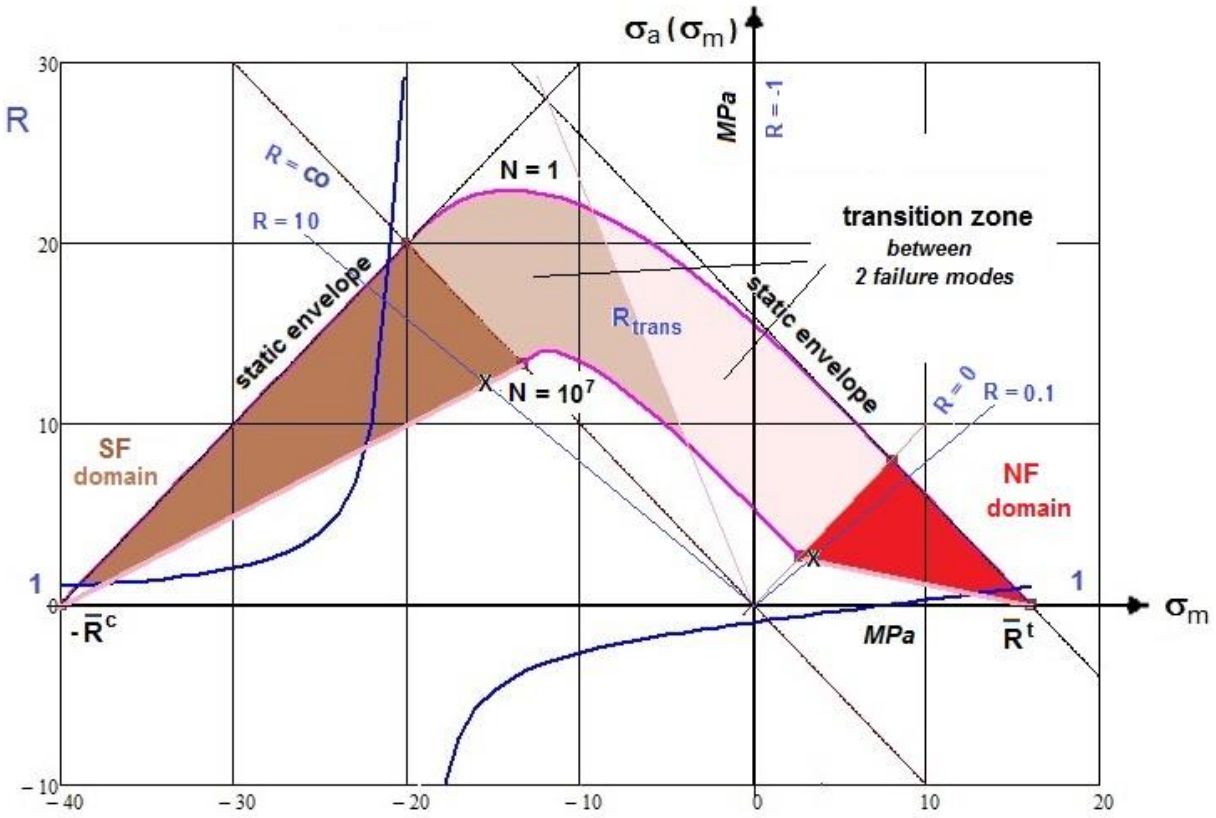


*Fig. 8: Schematic Haigh diagram of a brittle behaving I material experiencing two fracture failure types NF, SF and the course of the stress ratio* R ($\sigma_m$). *50% average mapping of data. Strengths* $R^t$, $R^c$. *NF = Normal Fracture, SF= Shear Fracture.*

In contrast to a ductility-driven damaging, where primarily one yielding failure mechanism reigns the damaging process from multi-axial stress states, in the brittle behaving case the material possesses more than one fracture failure mode. *Fig.8* presents a more schematic Haigh diagram for a brittle behaving isotropic material. The outer curve describes the static case where the static material stressing effort (Werkstoffanstrengung) *Eff* ($\sigma_m$, $\sigma_a$) becomes 100%. This is the same curve as $D(\sigma_m, \sigma_a, N = 1) \equiv Eff = 100\%$ and computed by employing the interaction formula $Eff = \sqrt[m]{(\Sigma\, Eff_{modes}{}^m)}$ in the transition zone with respect to the grading from one mode to the other, see Annex. For the constant life curves $D = 100\%$ is valid, too.
Viewing the large transition zone, it is mandatory to have R-curves in this zone, too. Hahne applied in [Hah15] R = 0.5 besides the standard stress ratios 0.1 in the tensile domain and R = 10 in the compressive domain.

The mode damaging driving uni-axial stress σ can be replaced by the mode-associated multi-axial equivalent stress $\sigma_{eq}$ (see Annex A and B). This means: (1) the 'uni-axial' equivalent stress value is damaging effect equivalent to the multi-axial stress state in the envisaged failure mode, and further, (2) a comparison with the failure mode–governing strength is possible (in German termed Vergleichsspannung).

***Of highest practical advantage for the user is the possibility to also use for the transversely-isotropic UD material equivalent stresses*** $\sigma_{eq}^{mode}$ ***similar to the ductile behaving materials (Mises)!***

## 5 Automatic Construction of Constant-Life Curves

### *5.1 Computation of CFL curves in the Haigh Diagram*

An automatic construction of failure-domain-linked Constant Fatigue Life (CFL) curves $\sigma_a$ ($\sigma_m$, $R$, $N$ = constant) in the Haigh Diagram would be a desired objective for the design engineers. This task can be solved for brittle behaving materials and for UD materials, too.

In the UD case exist 3 separate Haigh diagrams (2D): one for FF (FF1 tension with FF2 compression) and two for IFF, namely (IFF1 lateral tension with IFF2 lateral compression), and further IFF3 for in-plane shear. Including IFF3 into IFF1-IFF2, two 3D Haigh surfaces can be obtained $\boldsymbol{\sigma_{2a}(\sigma_{2m}, \tau_{21m})}$ and $\boldsymbol{\tau_{21a}(\sigma_{2m}, \tau_{21m})}$, see also [Wei11, Gai16] and chapter 5.4**.**

In chapter 4 it could be recognized that the prediction of further mode S-N curves by using the Basic (mode) S-N curve and Kawai's approach is generally effortful. However, for a suitable mapping of the course of S-N test data the mapping formulation must involve more parameters in order to map the usually non-linear curves. For normal practice it is recommended to choose the reduced Weibull model, mapping model 2 with three parameters plus tensile strength point $R_{||}^t$ (no bar over put here). A minimum error fit was intentionally not applied here but an analytical determination of the curve parameters: two anchor points X from the Basic S-N curve are employed to determine the extra S-N curve parameter of the chosen higher order mapping model 2.

For the running variable R and a fixed fracture cycle number $N$ the points ($\sigma_a(N)$, $\sigma_m(N)$) on the desired constant life curve parts are given for each failure mode domain (here demonstrated for FF1).

There are two possibilities to determine the Ψ curve parameters:

1. Firstly by classically determining the Basic S-N curve with a sufficiently mapping model with determination of the parameters of the $\Psi$ model by using two anchor points at $10^4$ and $10^7$ of the respective Basic S-N curve in order to compute the free Ψ curve parameters (chosen possibility here). This leads via (example FF1)

   * Choice of Basic S-N model

   * $\Psi_t = \sigma_a / ( R_{||}^t - \sigma_m ) = 0.5 \cdot (1\text{-}R) \cdot \sigma_{max} / [ R_{||}^t - 0.5 \cdot (\mathbf{1}+R) \cdot \sigma_{max}]$

   * * Determination of $\sigma_{max}^{pred}(N,R) = (2 \cdot R_{||}^t \cdot \Psi_{master}) / [ \Psi_{master} - R + R \cdot \Psi_{master} + 1]$.

2. Directly fitting the Basic S-N curve data points by the chosen $\Psi$ mapping model.

   * Choice of Ψ mapping function , e.g. $\Psi_{master}(N) = c_{\Psi 1} + (1 - c_{\Psi 1}) / \exp(\frac{\log(N)}{c_{\Psi 3}})^{c_{\Psi 1}}$

   * Determination of $\sigma_{max}^{pred}(N,R) = (2 \cdot R_{||}^t \cdot \Psi_{master}) / [ \Psi_{master} - R + R \cdot \Psi_{master} + 1]$.

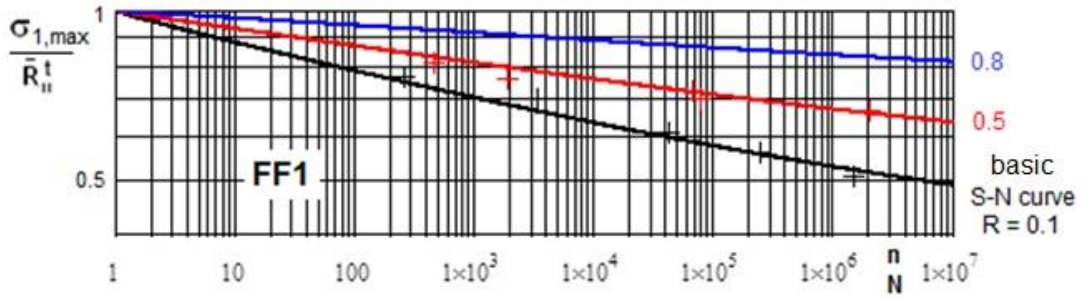


*Fig. 9: Predicted log-log FF1 S-N curves* R = 0.5, 0.8 *after Kawai. Mapping model* 5

With the computed max curve for R = 0.1 or min curve for R = 10 the mean stress as well as the amplitude stress can be calculated by using

$$\sigma_m{}^{pred}(N) = \frac{\sigma_{\max}{}^{pred}(N) + \sigma_{\max}{}^{pred}(N)}{2} \quad , \quad \sigma_a{}^{pred}(N) = \frac{\sigma_{\max}{}^{pred}(N) - \sigma_{\max}{}^{pred}(N)}{2} \cdot \quad (6)$$

Note: *As the Kawai's $\Psi$ approach does not yet sufficiently well describe the intermediate mode S-N curves his approach must be 'tuned' in future on a broader basis of test data.*

### *5.2 Solution procedure for obtaining CFL curves in the IFF1 - IFF2 Transition Zone*

No problem existed to derive Haigh Diagrams FF and IFF3 in the case of strength values of similar size: Then, the static interaction formula below could be used due to

$$Eff = [(Eff^{NF})^m + (Eff^{SF})^m]^{m^{-1}} = 100\% = 1 \quad (7)$$

$$\left(\frac{-(\sigma_{2m} - \sigma_{2a}) + |\sigma_{2m} - \sigma_{2a}|)}{2 \cdot \overline{R}_\perp{}^c}\right)^m + \left(\frac{\sigma_{2m} + \sigma_{2a} + |\sigma_{2m} + \sigma_{2a}|)}{2 \cdot \overline{R}_\perp{}^t}\right)^m = 1.$$

the fact that $-R^c/\,R^t \equiv R_{trans} \approx -1$ which means the alternating stress ratio is about the transition zone dominating stress ratio $R_{trans}$. The absolute brackets are helpful when senseless negative *Effs* must be avoided. Above procedure with the interaction formula numerically works for $N = 1$, delivering the CFL curve for $N = 10^0 = 1$, considering both NF + SF in the transition zone. However recalling, a problem arises when strength values are very different, for $R \approx >1.5$.

Hence, for the IFF1-IFF2 Haigh Diagram a new solution procedure had to be investigated for higher N:

*Assumption: *The failure mode domain terminates at the beginning of the other mode domain, for instance IFF1 at IFF2 and vice versa. An exponential decay is used.*

*Interaction formula, engineering-like adapted as function of $N$ (index $_N$):

$$\sigma_{a,N}(\sigma_m) = \left[\left(\frac{\sigma_{aSF,N}(\sigma_m)}{1 + e^{\frac{c_{1SF} + \sigma_m}{c_{2SF}}}}\right)^m + \left(\frac{\sigma_{aNF,N}(\sigma_m)}{1 + e^{\frac{c_{1NF} + \sigma_m}{c_{2NF}}}}\right)^m\right]^{1/m} \quad \text{with straight lines} \quad (8)$$

$$\sigma_{aSF,N}(\sigma_m) = c_{1aSFs,N} + c_{2aSFs,N} \cdot \sigma_m \;,\; \sigma_{aNF,N}(\sigma_m) = c_{1aNFs,N} + c_{2aNFs,N} \cdot \sigma_m$$

The straight lines (index $_s$) are drawn from the strength point to the associated X anchor point on the Basic mode S-N curve in Fig.10.

For SF, from R = ∞ or from the anchor point X of R =10 (down to zero at the 'end' of the NF domain. For NF, the procedure is the other way round with R = 0 or with R = 0.1. All anchor points X are computed from S-N mapped test data courses, where the Basic S-N curve is one thereof.

The CFL curves are derived by the application of the formulas above when inserting R as running variable and setting $N$ = constant to obtain a distinct CFL curve and numerically resolving for $N = 10^4$ or $10^7$. This works for other Haigh Diagrams the same.

As can be seen in the respective Haigh Diagrams, the CFL curve – originally straight – still bends from the X location on.

CFL curves for IFF1-IFF2 Haigh diagram, drawn through both the failure domains and the transition zone are the achieved desired result. This means: ***Failure mode-linked constant fatigue life (CFL) curves $\sigma_a$ ($\sigma_m$, R, $N$ =*** constant***) can be automatically computed.***

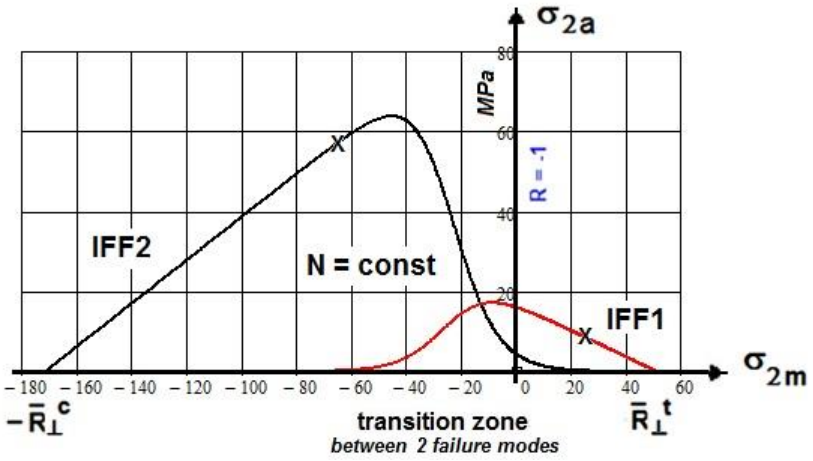


*Fig.10: Schematic visualization of the assumed exponential decay, anchor points* X *from Basic S-N curves* R = 0.1, 10,

## 6 Generation of the UD modes'–linked Haigh Diagrams

### *6.1 The IFF3 Diagram, $\tau_{21} \equiv \sigma_{eq}^{\perp\parallel}$*

Two S-N curves are provided in *Fig. 11* for the establishment of the IFF3 Haigh diagram. The origin value for R = - 1 must be $\leq \bar{R}_{\perp\parallel}$ . The estimation is, due to the following derivation,

$$\left(\frac{\sigma_{fr,-1}}{\bar{R}_{\perp\parallel}}\right)^m + \left(\frac{|\sigma_{fr,-1}|}{\bar{R}_{\perp\parallel}}\right)^m = 1\,,\ \left(\sigma_{fr,-1}\right)^m + \left(\frac{\sigma_{fr,-1}\cdot\bar{R}_{\perp\parallel}}{\bar{R}_{\perp\parallel}}\right)^m = \left(\bar{R}_{\perp\parallel}\right)^m,\ \ \sigma_{fr,-1} = \left(\frac{\bar{R}_{\perp\parallel}{}^m}{1+1}\right)^{1/m},$$
$$\sigma_{fr,-1} = \left(\frac{\bar{R}_{\perp\parallel}{}^m}{2}\right)^{1/m} = 48.3\,\text{MPa} < \bar{R}_{\perp\parallel} = 70\,\text{MPa}. \qquad (9)$$

The R = -1 curve was not tuned according to the meager number or test results. It shall be just document the different course from the origin N = 1 onward into the HCF domain

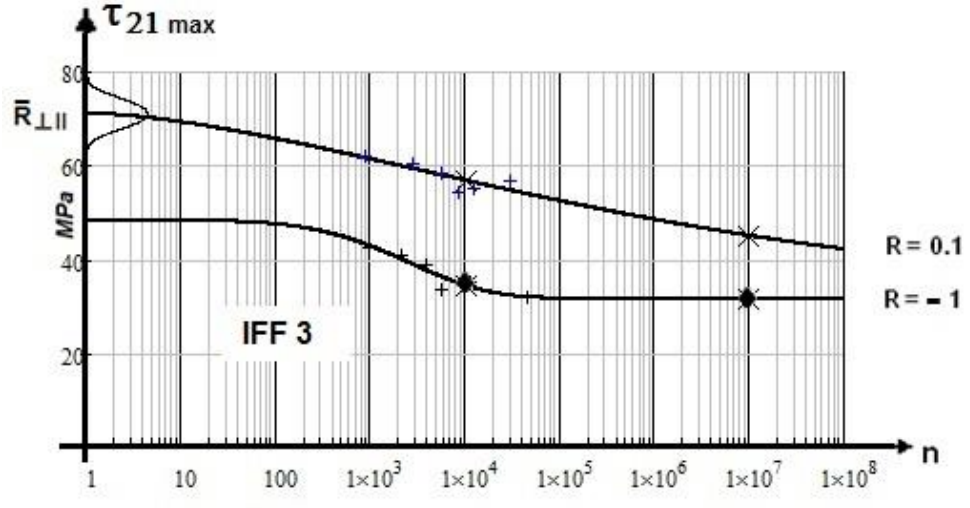


*Fig.11: Log-log IFF3-linked S-N curves [data, courtesy C. Hahne], anchor points* X *at N = $10^4$, $10^7$.*

♦ *Kawai approach- check point from tested non-basic S-N curve* R = -1

As the first Haigh diagram the FF3 diagram shall be provided.

The S-N curve $N$ =1 is determined according to the interaction formula of the twofold acting static mode IFF3 or - in other words - the same mode acts twofold under R = -1. The

determining $Eff$ reads - in the simple case $Eff^{\perp\|} = \tau_{21} / R_{\perp\|}$, that is inserted into

$$(Eff^{\perp\|})^m + (Eff^{\perp\|})^m = \left( \frac{-(\tau_{21m} - \tau_{21a}) + |\tau_{21m} - \tau_{21a}|)}{2 \cdot R_{\perp\|}} \right)^m + \left( \frac{(\tau_{21m} - \tau_{21a}) + |\tau_{21m} - \tau_{21a}|)}{2 \cdot R_{\perp\|}} \right)^m = 1 = 100\% \cdot$$

Above interaction formula captures the two plain failure domains (positive and negative shear stress mode) and the transition zone as well. For $N = 10^0 = 1$ the basic strength $R_{\perp\|}$ (blue dot) is 70 MPa. $R_{\perp\|}$ must be replaced for larger $N$ by the $N$-associated residual strength $\sigma_{res}(N, \sigma_m)$, e.g. here exemplarily $\sigma_{max}$ at $N = 10^5$ and at $N = 10^7$ cycles marked by a cross X on the S-N curves in *Fig.11*.

For the static strength replacing residual strength a linear corrective relationship was assumed to be sufficient in the two symmetric mode domains, such as for $N = 10^4$ cycles, indicated by $^{(4)}$ in $R_{\perp\|}^{(4)}$

$$R_{\perp\|} + \tau_{21a}^{(4)} \cdot (R_{\perp\|} - R_{\perp\|}^{(4)}) / (\tau_{21aN}^{(4)}) \quad . \qquad (10)$$

Usually, S-N tests deliver values for the standard stress ratios R = 0.1 and R = 10 which are mapped according to the previously given S-N data mapping functions. Therefore, the X-points are computed with the mapping function model and taken here as bounding values of the two modes. Two S-N curves were provided for the establishment of the IFF3 diagram, *Fig.9*.

For assessing the quality of the predicted curves checking points ♦ are computed from all the mapped S-N curves (more than the Basic S-N curves have been mapped) and depicted in the Haigh Diagrams as local quality indicators. One must dedicate the check points to the chosen CFL curves $N = 10^5$ and at $N = 10^7$ since the test data are seldomly lying on these curves.

*<u>Notes</u>: (1) Whereas here in the Haigh diagram the constant life curve part - within the transition zone - was the damaging result of a twofold active mode at* R = -1 *in the following diagrams it is the damaging result of different modes. (2) Strength failure conditions (criteria) regularly describe just one occurrence of a failure mode linked to one failure mechanism. Therefore, a twofold acting mode, such as $\sigma_2 = \sigma_3$, with its higher damaging effect must be regarded on top. (3) The interaction at* R = -1 *- $\tau_{21}$ with + $\tau_{21}$ corresponds to the equi-bi-axial stress state $\sigma_2 = \sigma_3$ in the quasi-isotropic $\sigma_2$-$\sigma_3$-plane of the UD material.*

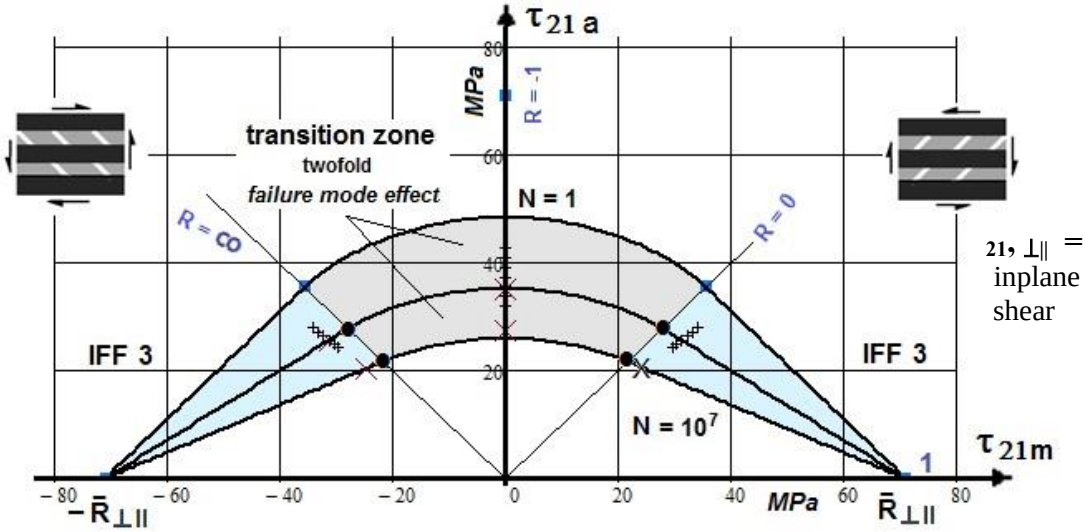


*Fig.12: IFF3 Haigh diagram (a:= amplitude, m:= mean, N := number of fracture cycles,* R= *$\sigma_{min}/\sigma_{max}$). Test data CF/EP, courtesy [Hah14],* X = *anchor point, • predicted mode domain boundary point, ♦ Kawai approach- check point from tested non-basic S-N curves*

### *6.2 The FF1-FF2 Diagram, $\sigma_1$, $\sigma_{eq}^{\parallel\sigma}$, $\sigma_{eq}^{\parallel\tau}$*

Four S-N curves are provided and presented as lin-log plots in *Fig.13* for the establishment of *Fig.14*. As points indicated are the anchor points on R = 0.1 and 10. Further indicated there are the check points ♦ for testing the prediction capability of the Kawai model, always having in mind that scatter will never fully allow a full prediction however improve an estimation. The CFL curves in *Fig.14* run through the X-points and approximately map the associated check points ♦ on the R = 0.5 (≠ Basic S-N curve). It must be further noted that the test samples' size was pretty small for a fair validation of the modeling method.

Essential for the lifetime prediction of multi-axial laminates is the determination of FF-damaging of the embedded lamina by a provided FF1-FF2 Haigh diagram. The outer bounding curve is determined according to the interaction formula of the two modes FF1 (NF) and FF2 (similarity to SF). This formula reads in the 2D case (11)

$$Eff = (Eff^{\parallel\sigma})^m + (Eff^{\parallel\tau})^m = \left(\frac{-(\sigma_1-\sigma_{1a})+|\sigma_{1m}-\sigma_{1a}|)}{2\cdot\bar{R}_{\parallel}^{\,c}}\right)^m + \left(\frac{\sigma_{1m}+\sigma_{1a}+|\sigma_{1m}+\sigma_{1a}|)}{2\cdot\bar{R}_{\parallel}^{\,t}}\right)^m = 1 = 100\,\%.$$

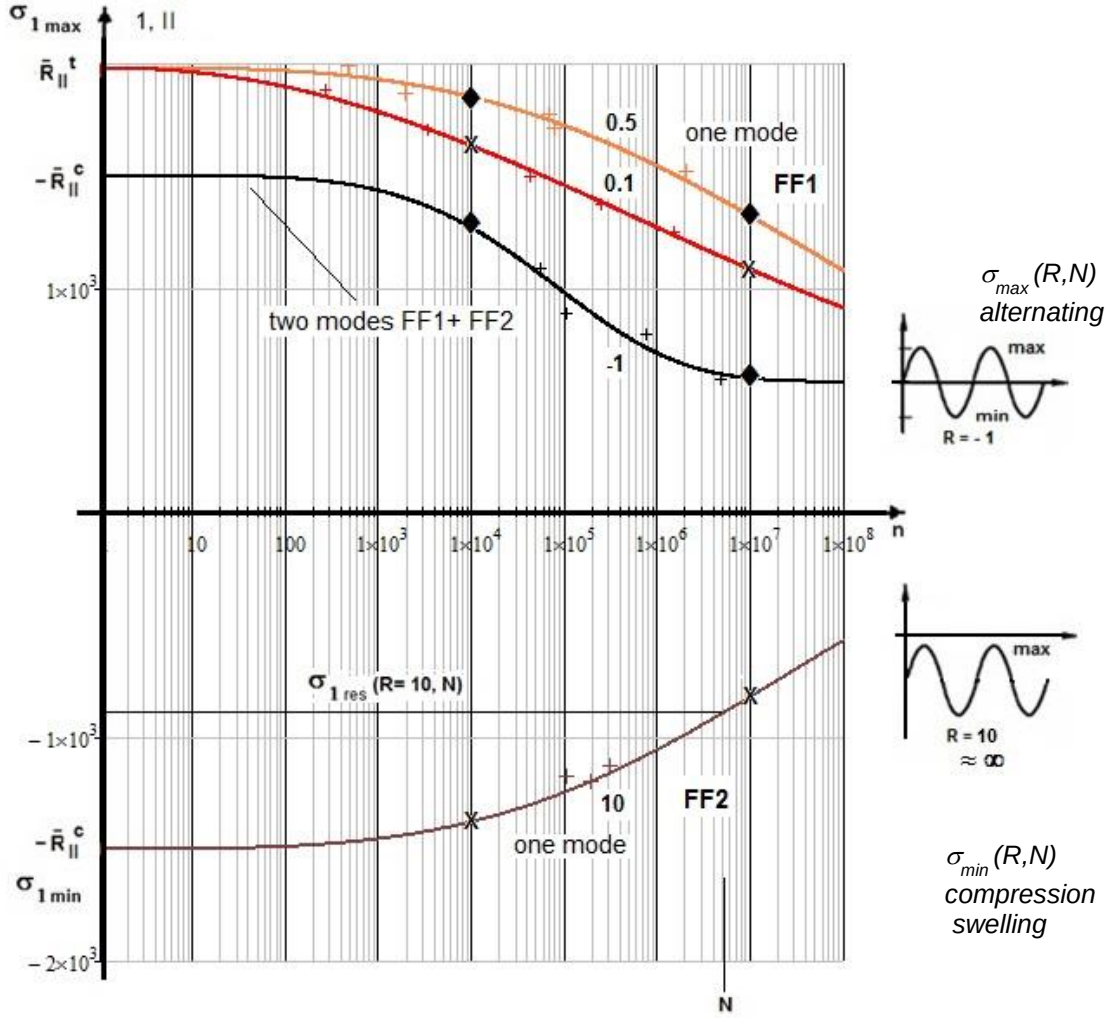


*Fig. 13: Lin-log FF1-FF2-linked S-N curves [data, courtesy Kawai, Suda], analytically determined characteristic anchor points X , • predicted mode domain boundary point, ♦ Kawai approach- check point from tested non-basic S-N curves* R = 0.5, -1

It involves both, the two pulsating domains and the transition zone as well, being the joint action domain of both the modes FF1 and FF2. Again, the absolute formulation keeps senseless negative *Effs* away. The CFL curves in *Fig.14* approximately map the associated points ♦ on the R = 0.5 curve.

Note: Principally, also for $N$ = 1, the R = -1 curve is the result of two damaging portions stemming from tension and compression, determinable by the following interaction equation

$$\left(\frac{\sigma_{fr,-1}}{\bar{R}_{\parallel}{}^{t}}\right)^{m}+\left(\frac{|\sigma_{fr,-1}|}{\bar{R}_{\parallel}{}^{c}}\right)^{m}=1\,,\left(\sigma_{fr,-1}\right)^{m}+\left(\frac{\sigma_{fr,-1}\cdot\bar{R}_{\parallel}{}^{c}}{\bar{R}_{\parallel}{}^{t}}\right)^{m}=\left(\bar{R}_{\parallel}{}^{c}\right)^{m},\quad \sigma_{fr,-1}=\left(\frac{\bar{R}_{\parallel}{}^{t\,m}}{1+\bar{R}_{\parallel}{}^{t\,m}/\bar{R}_{\parallel}{}^{c\,m}}\right)^{1/m}\quad,\ (12)$$

see *Fig.13.* This delivers a lower bound for $\sigma_{fr,-1}$ = 1276 MPa, that is to compare to the two strength levels of 1980 MPa for tension and of 1500 MPa for compression. The value must be smaller than the smaller strength, which here means $\bar{R}_{\parallel}{}^{c}$ which is simply applied here as origin. This treatment is principally valid despite of the fact that measured S-N data might be higher than $\sigma_{fr,-1}$ for lower values of $N$ and that the proven experience says "in accurate strength measurements tensile UD strength and compressive UD strength become practically the same size", which physically means the compressive strength is a instability result.

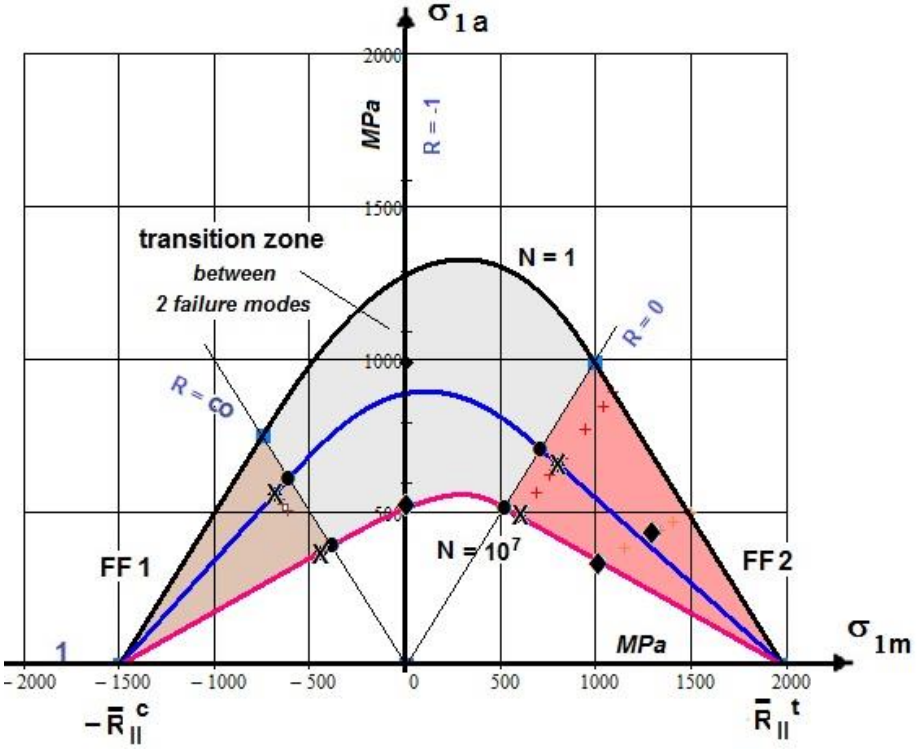


*Fig. 14: FF1-FF2 Haigh diagram, displaying the failure mode domains, transition zone, test data [Hah14].Anchor point X , • predicted mode domain boundary point, ♦ Kawai approach-check point from tested non-basic S-N curves* R = 0.5, -1

Notes: *(1)As with the static case, also here, for general stress states the cylic stresses in the Haigh diagrams may be replaced by the associated equivalent stresses. (2) A reliable modeling depends on the size of provided reliable test data.*

### *6.3 The IFF1-IFF2 Diagram, $\sigma_2$, $\sigma_{eq}{}^{\perp\sigma}$, $\sigma_{eq}{}^{\perp\tau}$*

Four S-N curves are provided in *Fig 15* for the establishment of *Fig.16*. The basic S-N curves are R = 0.1 and 10. From them the associate $\Psi$-function is determined.

Now, the IFF1-IFF2-Haigh diagram can be determined, *Fig.16.* This figure represents an in-plane Haigh diagram. The outer bounding curve is statically determined (N=1) according to the interaction formula of the two modes IFF1 and IFF2. This formula reads in the 2D case

$$(Eff^{\perp\sigma})^m + (Eff^{\perp\tau})^m = \left(\frac{-(\sigma_{2m}-\sigma_{2a})+|\sigma_{2m}-\sigma_{2a}|)}{2\cdot R_\perp{}^c}\right)^m + \left(\frac{\sigma_{2m}+\sigma_{2a}+|\sigma_{2m}+\sigma_{2a}|)}{2\cdot R_\perp{}^t}\right)^m = 1. \quad (13)$$

The origin value for R = - 1 must be $\leq \bar{R}_\perp{}^t$.

Whereas R = -1 is tension-driven, the S-N curve $R_{trans}$ is equally driven by both the modes. The application of the interaction equation delivers for R = -1 and $R_{trans}$= -3.4

$$\left(\frac{\sigma_{fr,-1}}{\bar{R}_\perp{}^t}\right)^m + \left(\frac{|\sigma_{fr,-1}|}{\bar{R}_\perp{}^c}\right)^m = 1\,,\left(\sigma_{fr,-1}\right)^m + \left(\frac{\sigma_{fr,-1}\cdot\bar{R}_\perp{}^c}{\bar{R}_\perp{}^t}\right)^m = \left(\bar{R}_\perp{}^c\right)^m,\ \sigma_{fr,-1} = \left(\frac{\bar{R}_\perp{}^{tm}}{1+\bar{R}_\perp{}^{tm}/\bar{R}_\perp{}^{cm}}\right)^{1/m}$$
$$\left(\frac{\sigma_{fr,tr}}{\bar{R}_\perp{}^t}\right)^m + \left(\frac{|\sigma_{fr,tr}|}{\bar{R}_\perp{}^c}\right)^m = 1\,,\left(\sigma_{fr,tr}\right)^m + \left(\frac{\sigma_{fr,tr}\cdot\bar{R}_\perp{}^c}{\bar{R}_\perp{}^t}\right)^m = \left(\bar{R}_\perp{}^c\right)^m,\ \sigma_{fr,trans} = \left(\frac{\bar{R}_\perp{}^{tm}}{1+\bar{R}_\perp{}^{tm}/\bar{R}_\perp{}^{cm}}\right)^{1/m}, \quad (14)$$

fracture stresses at the origin *N*=1 of $\sigma_{fr,-1}$= 50.1 MPa and $\sigma_{a,trans}$ = 84 MPa ($R_{trans}$ = -3.4 : 1; max$\sigma_{fr,trans}$ = 38.5 MPa, min$\sigma_{fr,trans}$ = -130.9 MPa, $\sigma_{m,trans}$= -46.2 MPa,).

For the computation of the CFL-curves of N = $10^5$ (here just for $10^5$, test data for R = 10 were available) and $10^7$ cycles the numerical computation of the CFL curve parts in the transition zone did not yet work because the strength values are so different in size.. A new solution procedure was prepared, see chapter 5.2.

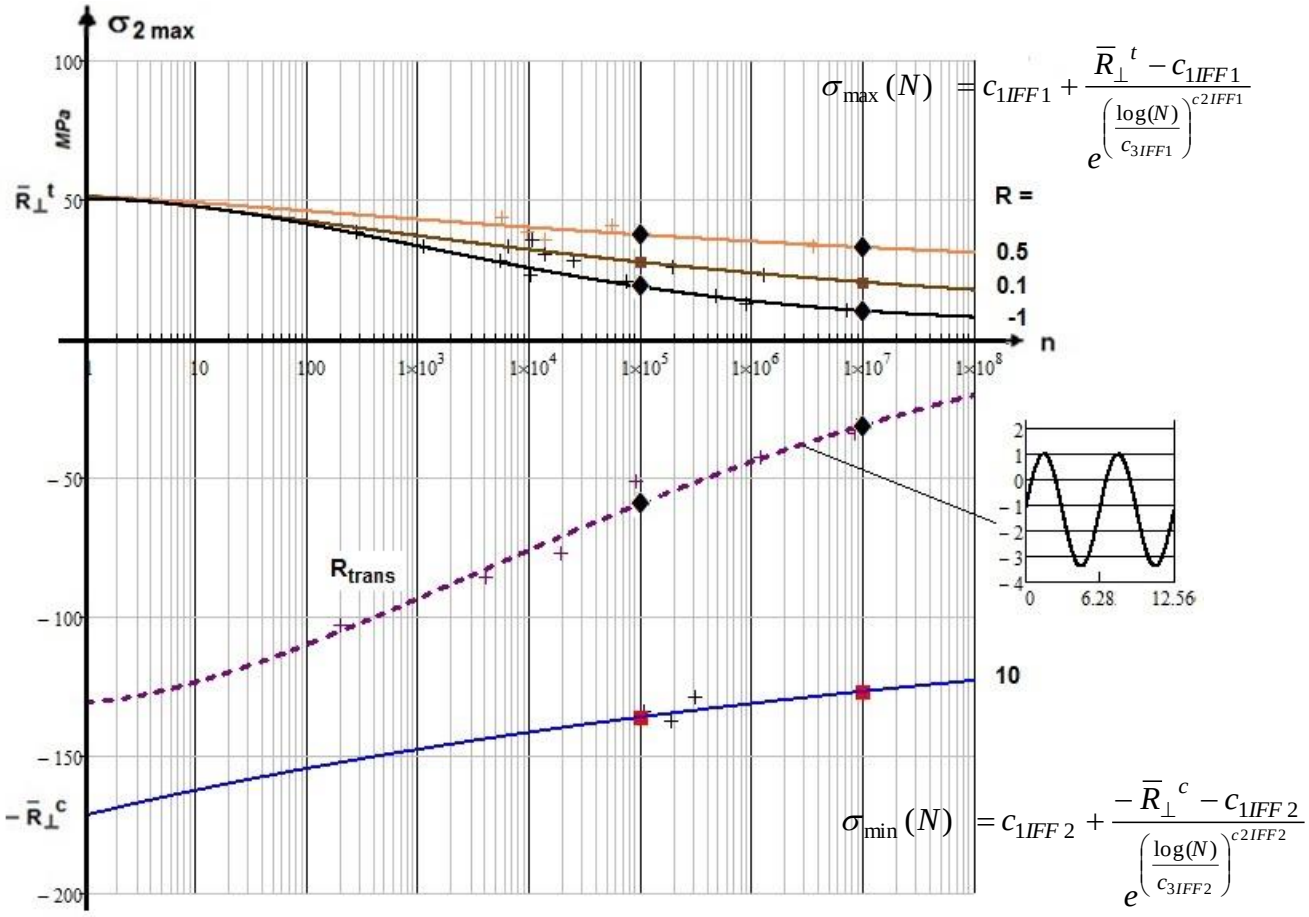


*Fig.15: Lin-log IFF1and IFF2-linked S-N curves [data, courtesy C. Hahne]*

Curves in the IFF1 domain are non-linear and in the IFF2 domain not really known! Check points from $\Psi$-prediction lie higher than points from S-N test data evaluation (to be improved in future investigations).

In the 'usual' case of multi-axial stress states, the IFF-associated uni-axial stress $\sigma_2$ is replaced by the IFF-associated equivalent stress $\sigma_{eq}^{\perp}$ (see Annex A).

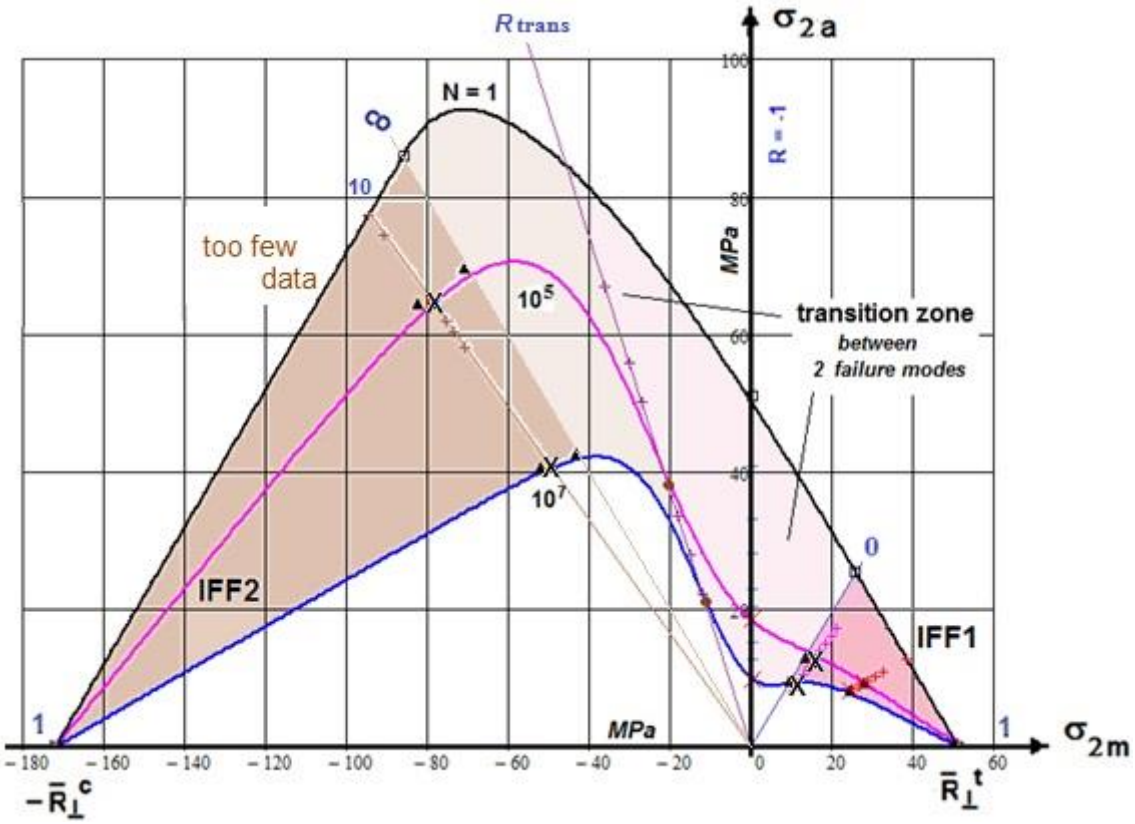


*Fig.16: IFF1-FF2 Haigh diagram, displaying the failure mode domains, transition zone, test data [Hah14] and the Basic S-N curve computed X-points as anchor points for the predicted CFL curves*

### *6.4 The 3D-IFF Haigh Surfaces $\sigma_{2a}(\sigma_{2m}, \tau_{21m})$ and $\tau_{21a}(\sigma_{2m}, \tau_{21m})$, proportional loading*

The Haigh diagrams for UD materials can be reduced to the 2D-FF Haigh diagram and a composed 3D-IFF diagram for the 2D stress state ($\sigma_2$, $\tau_{21}$) or the respective $\sigma_{eq}$-stresses for the general state. In the latter case the constant fatigue curves are replaced by constant fatigue surfaces. The presumption to perform this in the above way is *proportional loading*!

The static strength failure interaction condition reads

$$Eff = [(Eff^{IFF1})^m + (Eff^{IFF2})^m + (Eff^{IFF3})^m]^{m^{-1}} = 100\ \% . \qquad (15)$$

Further the equations (8) hold.

The complicated calculation did not yet fully work, the program must be reworked to obtain stabile numerical solutions in the transition zone. The figure below is a first trial showing the just the parts where the mode domains are..

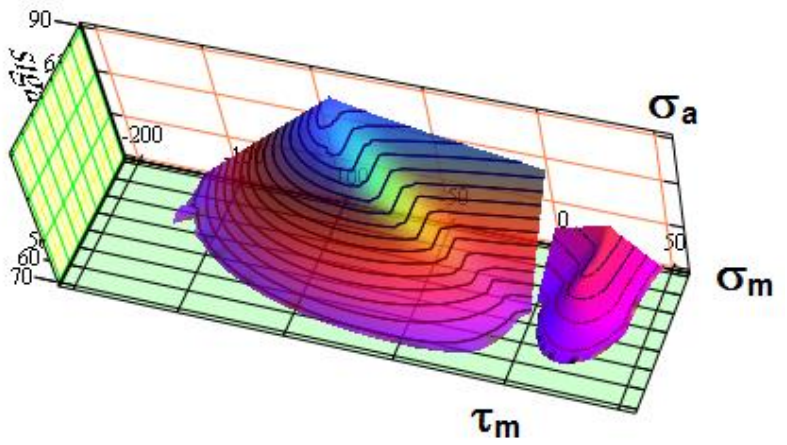


*Fig. 17: The 3D IFF (IFF1-IFF2-IFF3) Haigh Surface $\sigma_{2a}(\sigma_{2m}, \tau_{21m})$*

## 7 Cuntze's Fatigue Life Model with Numerical Application and Visualization

### *7.1 General*

In cyclic design case the required lifetime could be principally demonstrated by

$$RF_{life} \approx \frac{\text{Predicted Lifetime}}{j_{life} \cdot \text{Design Limit Lifetime}} > 1 \qquad (16)$$

with $j_{life} > 5$ (>> $j_{static}$). After cyclic degradation, caused by operational loading (< DLL), it must be demonstrated that the residual (static) strength is high enough to sustain Design Ultimate Load DUL (e.g. in spacecraft, DUL = $j$ult · DLL). An important feature is the demonstration of the residual strength at DUL level for the fixation of the replacement time procedure and at DLL level for the inspection method. For the designer, an important point in aircraft became the possibility to use a certification 'by analysis supported by tests' which saves time and much test costs.

In fatigue life estimation models many challenges must be mastered. A first challenge in the *Fatigue-life-model,* that applies S/N curves, is that it requires many test data. In order to reduce the associated test effort, it would be very effective - also in the sense of the BeNa agreement - to perform a lifetime prediction for a laminate on basis of an *in-situ master lamina S/N curve* for each single failure mode. Further S/N curves for the same failure mode, required in fatigue analysis, can be predicted from the basic S-N curve by utilizing the classical strain energy equality principle or much better Kawai's model, applied for UD material, see [Hah14, Cun16, 09]. This enables the engineer in pre-dimensioning to build lifetime predictions for variable loading in tension, shear and compression on a cheaper basis. There is some hope that at least for fiber-dominated laminates an embedded (in-situ) lamina fatigue design may replace the laminate design.

Formally, the same procedure is applied as for the usually ductile behaving metals. However, physically much better fits a dedication to brittle behaving metals (e.g. grey cast iron) since these are more related to the usually brittle behaving composite materials. They also experience two different fracture failure modes under tension NF and under compression SF. Ductile behaving metals, however, experience the same yielding failure mode under tension, shear or compression. whereby the so-called mean-stress effect is much smaller.

*Notes: (1) Stress (not strain) SFCs are applied to determine the subsequent damaging portions: They capture the combined effect of lamina stresses and consider residual stresses from manufacturing cooling down (essential for HCF). Stress SFCs cannot be used if*

*straining is caused in a distinct zero stress direction (examples $\sigma_I = \sigma_{II}$ (isotropic) or $\sigma_1 = \sigma_2$ (UD). This situation must be considered in a macroscopic SFC (as in the author's UD SFCs). (2) Because semi-brittle and brittle behaving materials experience several failure modes or failure mechanisms this has the consequence:* ***More than one strength failure condition (criterion) must be employed when modeling!*** *(3) Presumption for an application of static criteria is that the fracture failure modes are the same statically and cyclically.*

Now, the author's basic and partly novel ideas of his approach are presented in detail.

### *7.2 Steps of the Full Approach, example FF*

***Step 1: Novel Modeing of loading cycles***

Assumption: Associated rainflow counting possible

For the sake of simplicity - for displaying the load modeling idea in the figure below - an isotropic brittle material is taken with a stress ratio $R$ = -1. This idea was still proposed in 1996 by the author [Cun96]. The idea requires a *failure mode-linked apportionment of cyclic loading* (better termed here stressing as the finally used derivative of the loading). Of course, this idea will finally lead to a mode-related accumulation of the damaging portions.

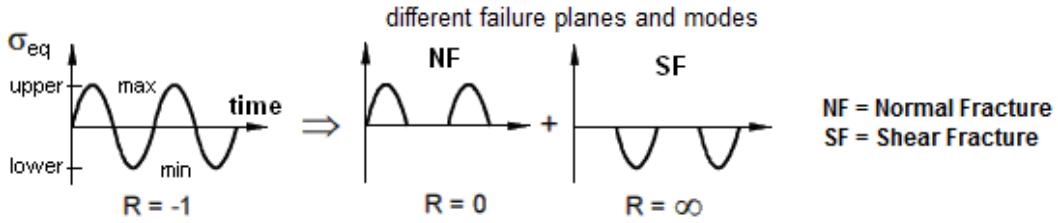


***Step 2: Measurement and simple Modeling of Basic and to-be-predicted S-N curve (FF1)***

Assumption: Mapping of the course of test data is possible by a mapping curve, e.g.

$$\sigma^{master}_{\parallel,\ max}(N) = \sigma^{R=0.1}_{\parallel,\ max}(N) = \overline{R}^{t}_{\parallel} \cdot N^{c_{master}} \quad , \quad \sigma^{pred}_{\parallel,\ max}(N) = \overline{R}^{t}_{\parallel} \cdot (N)^{c_{pred}}$$

Above example delivers *a straight line in the log-log diagram and* minimizes the calculation effort.

***Step 3: S/N curve prediction by using M. Kawai's 'Modified Fatigue Strength Ratio'***

Assumptions: (1) Kawai's model is valid. (2) For the calculation of the damaging portions the 5 FMC-based static UD SFCs can be applied.

***Step 4: Mode–associated accumulation of the damaging portions*** $D_{\parallel},\ D_{\perp},\ D_{\perp\parallel}$

Assumption: Palmgren–Miner 'rule' is applicable.

The accumulation of damaging portions is performed by employing Palmgren-Miner's rule for the embedded lamina - cycle-wise, block-wise or otherwise -, however, considering the stress-state-failure mode relationship.

***Step 5: Automatic generation of CFL curves in Haigh diagrams and IFF Surface***

Assumption: Specific interaction that numerically works even for strength ratios R ≈ > 1.5.

With a computed maximum curve (or min curve for R = 10), Step 3, the predicted S-N curve reads

$$\sigma^{pred}_{\max}(N) = \overline{R}_{\parallel} \cdot N^{c1\,pred} \quad , \quad \sigma^{pred}_{\min}(N) = R \cdot \sigma^{pred}_{\max}(N) \ .$$

Then, due to the mean stress formulation, mean stress as well as amplitude stress can be calculated by using

$$\sigma_m{}^{pred}(N) = \frac{\sigma^{pred}_{\max}(N) + \sigma^{pred}_{\min}(N)}{2} \quad , \quad \sigma_a{}^{pred}(N) = \frac{\sigma^{pred}_{\max}(N) - \sigma^{pred}_{\min}(N)}{2} \ .$$

For the running variable, the stress ratio R, and a fixed cycle number $N$ continuous CFL-points $\sigma_a(N)$, $\sigma_m(N)$ are given for each failure mode domain, which was here demonstrated for FF1.

In this context, another numerical evaluation procedure of ($\sigma_a$, $\sigma_m$, R) test data sets shall be mentioned: In [Wei15] the complete test data set, that forms the full 3D failure surface, is mapped by Tschebyscheff-Polynomials. Thus, the plane Haigh Diagram with its $N$ = constant curves in the 2D plane becomes tri-axially with $N$ as space parameter building $N$ = constant curves on a 3D failure surface.

### *7.3 Visualisation by an Example FF Lamina under Variable Amplitude Loading*

Eventually, in *Fig.18* a schematic example is presented. Of course, a maximum allowable damaging value, a $D_{feasible}$, is to be derived *experimentally based.*

*Static strengths:* $\{\bar{R}\} = (2560,\ 1590,\ 73,\ 185,\ 90)^T\ MPa$,

*S/N curves:* $\sigma_{1,\max}^{R=0.5}(n) \approx \bar{R}_{\parallel}^{t} \cdot n^{-0.034}$, $\sigma_{\parallel,\ \max}^{R=0.1}(n) \approx \bar{R}_{\parallel}^{t} \cdot n^{-0.049}$ (basic S - N curve),

*Stresses:* $\{\sigma\} = (\sigma_1, \sigma_2, \sigma_3, \tau_{23}, \tau_{31}, \tau_{21})^T$, $\{\sigma_{eq}^{mode}\} = \left(\sigma_{eq}^{\parallel\sigma},\ \sigma_{eq}^{\parallel\tau},\ \sigma_{eq}^{\perp\sigma},\ \sigma_{eq}^{\perp\tau},\ \sigma_{eq}^{\parallel\perp}\right)^T$.

*Loadings:* $n_3(R = 0.1) = 0$,

$n_1(R = 0.1) = 100000\ cycles,\quad \sigma_1^{(1)} = 1250\ MPa,\quad N_1(R = 0.1) = 2300000\ cycles,$

$n_2(R = 0.1) = 1600\ cycles,\ \sigma_1^{(2)} = 1500\ MPa,\ N_2(R = 0.1) = 55000\ cycles,$

$n_4(R = 10) = 6000\ cycles,\ \sigma_1^{(4)} = -1150\ MPa,\ N_4(R = 10) = 50000\ cycles,$

$n_5(R = 0.5) = 600000\ cycles,\ \sigma_1^{(5)} = 1550\ MPa,\ N_5(R = 0.5) = 2600000\ cycles.$

*Damaging portions:* $D_{\parallel}$, $D_{\perp}$, $D_{\perp\parallel}$

$D = \sum n_i/N_i) = 100000/2300000 + 1600/55000 + 6000/5000 + 600000/2.600000 = 0.43.$

$MoS = (D_{feasible} / D) / (j_{Life} \cdot D) - 1 = [(0.8/0.43) / (3 \cdot 0.43)] - 1 = 0.4 > 0.$

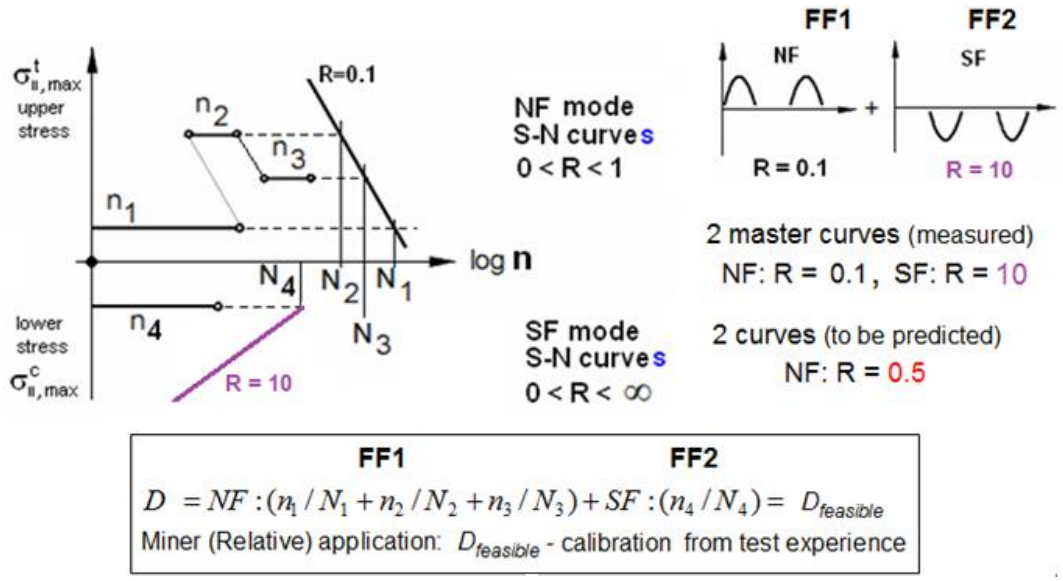


*Fig. 18: Schematic application of the method for the two FF modes*

### *7.4 Miscelleaneous*

***Manufacturing aspects:*** During manufacturing of composite parts residual stresses from curing and mounting may occur. An effect – leading to distortion – is warping or is spring-in. In the case of filling, compaction, curing and consolidation the performance of a process-

simulation delivers essential input for the structural analyses during design dimensioning. Matrix nesting and voids may be also generated. Since fiber orientation is essential for stiffness and strength the manufacturing process must be qualified and non-acceptable draping orientation and undulation minimized. The fiber direction must be straight, no waving within a layer and no waviness between layers.
Fatigue test results indicate that voids may have a strong detrimental effect on the fatigue life of composite structures if the void content is above a critical value. The grade of this detrimental effect depends on the laminate stack, loading condition, and activated stress states. It must be checked whether a project-required functionality of the composite part is not met or violated, respectively.

***Design for constant and variable amplitude loading***: In *Fig.19* the lifetime increasing variable amplitude loading (= fatigue life curve after Gaßner) of the structure in operation is displayed together with the harsher constant amplitude loading investigated in the chapters before. A loading spectrum-representing block-loading stands for a more realistic fatigue life estimation. Good information about the loading spectrum pays off.

***Interpolation between constant fatigue life (CFL) curves:*** In aircraft industry much effort is spent to determine intermediate constant–life curves, see for instance [HSB]. Therefore, an automatic possibility is highly desired in order to avoid difficult interpolations between the constant life curves.

***Mean stress corrections:*** For ductile behaving materials the Gerber theory is usually a good choice for ductile materials (strain life theory, LCF) and the Goodman theory may be a good model for brittle behaving materials (stress life theory). The Gerber theory treats negative and positive mean stresses the same whereas Goodman uses negative mean stresses, advantageous. Usually the loading is not fully reversed, hence a mean stress exists and should be accounted for by above corrective theories. Some fatigue data together with strength properties build the basis.

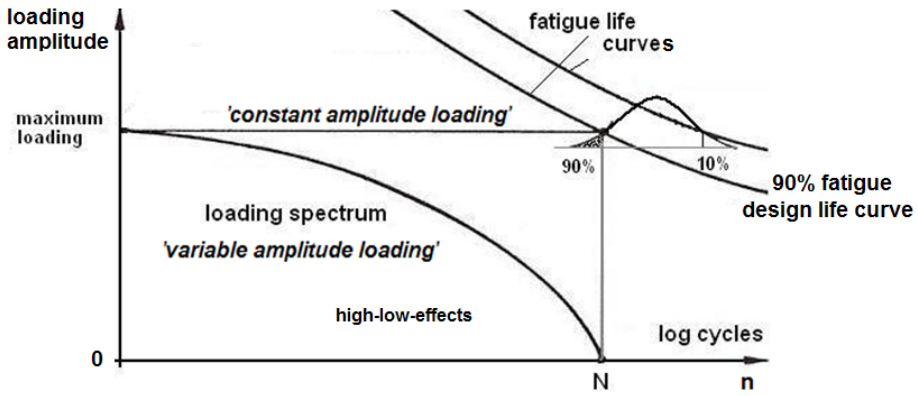


*Fig.19: Loading spectrum, variable and 'constant amplitude loading'*

***Proportional and non-proportional stressing (loading):*** Compared to proportional stressing non-proportional stressing (e.g. 90° out-of-phase) may lead to a significant life reduction. Due to the time-dependent, differently oriented stress state growing flaws have a better chance for coalescence viewing slip bands in ductile materials under strain-controlled fatigue testing or micro-cracks in brittle materials.

***Tackling uncertainties:*** Regarding the stack of laminas, a laminate is a random but not a deterministic failure system. As with other static and cyclic methods for laminates, the treatment of the "failure system laminate" composed of the "sub-failure systems of the

laminas" is not yet fully investigated. All the laminas of a laminate act together, and cause in-situ effects as well as a joint failure behavior. For instance, an IFF in one lamina (softening curve part is now to consider during the failure behavior) will follow a load redistribution which might make another lamina critical. For a better understanding, the associated degradation behavior should be investigated by employing structural reliability as it has been simply performed by the author still three decades before, see [Rac87]. The method practiced there is to transfer to not fully fiber-dominated lay-ups where all failure modes will contribute. Special situations such as non-proportional loading or not-in-phase loading may be tackled after having solved the basic reliability task.

## 8 Conclusions and Outlook for Brittle behaving Materials, especially UD material

### *8.1 Conclusions*

In order to reduce very costly cyclic laminate test programs the German Academic Research Group (BeNa) aimed at a Failure mode-based Lifetime Prediction Method, that should be 'embedded lamina-oriented in order to capture in-situ effects'. In this context an engineering method is proposed for a '*failure mode-based lifetime prediction for laminates'* (especially fiber-dominated ones) which employs the simple Relative Miner damaging accumulation rule. The proposed method looks like a 'macro-mechanical multiple mode damaging approach'. It avoids classical mean stress correction, and gives hope for a general treatment of laminates under variable loading.

Fatigue pre-dimensioning is possible: for 'well-designed', UD laminas-composed laminates by lamina dedicated FF- and IFF-linked, mode-representative S-N curves derived from sub-laminate test specimens, which capture the in-situ effect. Initial failure depends on the cycles-dependent shrinking of the IFF body determined by the degrading residual strength.

The Cuntze's Lifetime Prediction Method for UD laminas for the often fibre-dominated designed, UD lamina-composed high performance laminates consists of several steps:

1) Novel rigorous failure mode-linked load modelling (needs new rain-flow counting)
2) Measurement and mapping of a minimum number of mode-associated Basic S-N curves
3) Novel prediction of other necessary *mode S-N curves* on basis of the mode-associated Basic S-N curve and the mode-wise (the author's novel idea) application of *Kawai's 'Modified Fatigue Strength Ratio'*
4) Novel generation of failure mode-linked Haigh diagrams with a novel automatic generation of constant fatigue life curves (CFL). No mean stress correction is employed
5) Determination of damaging portions by applying 3D UD Static Failure Conditions ('criteria'). This depends on cycles-linked shrinking of the failure surface resulting in a smaller residual strength (for FF this is $R_{\|}$ ($R$, $N$)). The in-situ-effect of the embedded layer (physical lamina) is captured by deformation-controlled testing
6) Failure mode-related accumulation of damaging portions (novel idea) by using Relative Miner with previously determined damaging portions.

### *8.2 Outlook*

* The presented full approach still looks promising despite of the few test series available that could be used

* Effects of a negative 'neighbour-lamina notching' are seen to balance with a positive 'healing' effect due to redundant behavior since the layers are embedded.

* Deeper investigation of the novel idea and of probably not captured additional damaging caused by mode changes (FF, IFF, mixed) is required

* The FF applied method must be transferred to not fibre-dominated lay-ups where all failure modes such as IFF modes will contribute to composite part damaging

* Special situations such as non-proportional loading or not-in-phase loading must be tackled after having solved the basic task.

What needs to be further investigated?

- How essential mode interaction damaging really might be
- What can be done if interaction fracture failure test data in the associated transition domain is not available? This means, when missing R = - 1 and/or $R_{trans}$ (better), a guideline on the tests which should be performed at least
- Deeper investigation of the behavior in the transition domain with its joint damaging caused by mode changes (FF1 to FF2 at around $R_{trans}$) including crack-closure effects and investigation of IFF-caused fiber-notching effect
- How does the effect of loading sequence account for?
- Estimation of $D_{feasible}$ for pre-design from long-time experience on composite fatigue
- Applicability for further composite textile materials beside the classical multi-axial laminates and z-stitched non-crimped fabrics.

***Final Remarks:***

• Theory, 'only' creates a model of the reality, and experiment is 'just' one realization of the reality. Find a compromise to cost-optimally achieve a satisfying analysis-test verification procedure for a robust design and an excellent physically based correlation

• Physics have to be modelled accurately. All dimensioning load eases and failure modes must be accounted for

• Project task and deadline determine the model choice. In this context, the project must define what the essential project failures are

• Considering ‘short development time’, software should mature parallel to the present progress in manufacturing composite parts. Otherwise the expensive ‘Make and Test Method‘ cannot be reduced

• Quantitative measurement of degradation by NDI. This means for instance the measurement of sub-sequent micro-damaging in laminated walls. Controlling and monitoring are helpful uncertainty tackling measures

• When developing composite parts, holistic concurrent engineering thinking is more essential than with metals

• Loading sequence effects and overloading effects are not encountered here.

*<u>Note</u> on Design Requirements [from T.P. Sarafin, 1997]: (1) Functional requirements which describe what must be done, (2) Operational Requirements which describe how well it must be done, maximum tube deformation of 2 mm under a distinct rotational speed Ω), and (3) Constraints which limit the available resources, schedule, or physical characteristics such as tube length or maximum mass.*

*Author is in carbon business since 1970.*

**Literature** most literature found under *carbon~connected.de/Group/CCeV.Fachinformationen/Mitglieder*


[Ban16] Bansemir H.: *Certification Aspects*. Extended Abstract EC16, Augsburg 21-23. September 2016, conference publication

[Boe16] Boehm R., Thieme M., Koch I. and Gude M.: *Novel Materials Models and Multi-scale Simulation Methods for Composites*. EC16

[Chr13] Christensen R.M.: *The Theory of materials Failure*. Oxford University Press 2013, 143 pages

[Cun93] Cuntze R. and Heibel R.: *Increasing the usability of CFRP tubes by built-in-stresses*. Composite Structures 24 (1993), pp.251-264

[Cun96] Cuntze R.: *Bruchtypbezogene Auswertung mehrachsiger Bruchtestdaten und Anwendung im Festigkeitsnachweis sowie daraus ableitbare Schwingfestigkeits- und Bruchmechanikaspekte*. DGLR-Kongreß 1996, Dresden. Tagungsband 3

[Cun04] Cuntze R.: *The Predictive Capability of Failure Mode Concept-based Strength Criteria for Multidirectional Laminates*. WWFE-I, Part B, Comp. Science and Technology 64 (2004), 487-516

[Cun05] Cuntze R: *Is a costly Re-design really justified if slightly negative margins are encountered?* Konstruktion, März 2005, 77-82 and April 2005, 93-98 (reliability treatment of strength problem)

[Cun09] Cuntze R.: *Lifetime Prediction for Structural Components made from Composite Materials – industrial view and one idea*. NAFEMS World Congress 2009, Conference publication

[Cun11] Cuntze R.: *Tackling Uncertainties in Design – uncertain design parameters, safety concept, modelling and analysis.* Verbundwerkstoffe, GDM, 18. Symposium, Chemnitz 30.3. – 1.4. 2011

[Cun12 ]HSB 02000-01: *Essential topics in the determination of a reliable reserve factor*. 20 pages

[Cun13] Cuntze R.: *Comparison between Experimental and Theoretical Results using Cuntze's 'Failure Mode Concept' model for Composites under Triaxial Loadings - Part B of the WWFE-II*. Journal of Composite Materials, Vol.47 (2013), 893-924

[Cun14a] Cuntze R.: *The World-Wide-Failure-Exercises-I and –II for UD-materials – valuable attempts to validate failure theories on basis of more or less applicable test data*. SSMET 2014, Braunschweig, April 1 – 4, 2014, conference handbook

[Cun14b]: *Classical Laminate Theory (CLT) for laminates composed of unidirectional (UD) laminae, analysis flow chart, and related topics*. Reworked HSB 37103-01, Draft, 2014, 58 pages

[Cun15a] Cuntze, R.: *Reliable Strength Design Veriftcation - fundamentals, requirements and some hints*. 3rd. Int. Conf. on Buckling and Postbuckling Behavior of Composite Laminated Shell Structures, DESICOS 2015, Braunschweig, March 26 ~27, Ext. Abstract, Conf. Handbook, 8 pages

[Cun15b] Cuntze R.: *Bruchkörper in der Textilbetonbemessung für porösen Beton, Leichtbeton, UHPC und Lamelle – Wozu sind diese gut?* 7. Textilbetonanwendertagung Dresden 22.-23.9. 2015

[Cun16a] Cuntze R.: *Fracture failure surface of' the foam Rohacell 71G*. NAFEMS Regionalkonferenz , April 25-27, 2016, Bamberg.

[Cun16b] Cuntze, R.: *Introduction to the Workshop - from Design Dimensioning via Design Verification to Product Certification*. Extended Abstract, 9 pages, Experience Composites 2016, Augsburg, September 21-23

[Cun16c] Cuntze, R.: *Progress reached in UD Static Design and Lifetime Estimation*? Mechanik Kolloquium TU Darmsatdt, 21 Deec.2016. Extended presentation, 140 slides

[Gai16] Gaier C., Dannbauer H., Maier J. and Pinter G.: *Eine Software-basierte Methode zur Betriebsfestigkeitsanalyse von Strukturbauteilen aus CFK*. CCeV-Austria, AG Engineering, Meeting St. Martin im Innkreis, Sept.8. Magna-Powertrain, Engineering Center Steyr

[Geh09] Gehrig F., Mannov E. and Schulte K.: *Degradation of NCF-Epoxy Composites containing Voids*. ICCM 17, 27-31 July, 2009, Edinburgh

[Gud09] Gude W., Hufenbach W. and Koch I.: *Fracture Mode dependent Damage modelling of 3D Textile-reinforced Composites under Multi-axial Fatigue Loading*. ICCM 17, 27-31 July, 2009, Edinburgh

[Hah15] Hahne C.: *Zur Festigkeitsbewertung von Strukturbauteilen aus Kohlenstofffaser- Kunststoff-Verbunden unter PKW-Betriebslasten*. Shaker Verlag, Dissertation 2015, TU-Darmstadt,

Schriftenreihe Konstruktiver Leichtbau mit Faser-Kunststoff-Verbunden, Herausgeber Prof. Dr.-Ing Helmut Schürmann

[Hin16] Hinterhölzl R.: *MAI Design – Steps towards an Integral Design Approach from Process Simulation to Structural Analysis*. EC16

[Hoe16] Hoermann M.: *First-Ply-Failure and then What? – Approaches for detailed simulation of failure*. EC16

[HSB] German Aeronautical Technical Handbook *'Handbuch für Strukturberechnung*', issued by Industrie-Ausschuss-Struktur-Berechnungsunterlagen. TIB Hannover

[Kad13]Kaddour A. and Hinton M.: *Maturity of 3D failure criteria for fibre-reinforced composites: Comparison between theories and experiments*. Part B of WWFE-II, J. Compos. Mater. 47 (6-7) (2013) 925–966.

[Kaw04] Kawai M.: *A phenomenological model for off-axis fatigue behavior of uni-directional polymer matrix composites under different stress ratios*. Composites Part A 35 (2004), 955-963

[Koc16] Koch I., Horst P. and Gude M.: *Fatigue of Composites – The state of the art*. EC16

[Pet16] Petersen E., Cuntze R. and Huehne C.: *Experimental Determination of Material Parameters in Cuntze's Failure-Mode-Concept -based UD Strength Failure Conditions.* Submitted to Composite Science and Technology134, (2016), 12-25

[Puc02] Puck A. and Schürmann H.: *Failure Analysis of FRP Laminates by Means of Physically based Phenomenological Models.* Composites Science and Technology 62 (2002), 1633-1662

[Rac87] Rackwitz R. and Cuntze R.: *System Reliability Aspects in Composite Structures*. Engin. Optim., Vol. 11, 1987, 69-76

[Roh14] Rohwer K.: *Predicting Fiber Composite Damage and Failure*. Journal of Composite Materials, published online 26 Sept. 2014 (online version of this article can be found at: http://jcm.sagepub.com/content/early/2014/09/26/0021998314553885)

[Roos16] Roos R. and Devivier C.: *Strength and Curing Simulation of Thick-walled Composites with ANSYS WB 17.0*. EC16

[Sch06] Schürmann H.: *Konstruieren mit Faser-Kunststoff-Verbunden*. Springer-Verlag 2005

[Sch94] Schulte K.: *Compressive Static and Fatigue Loading of Continuous Fiber Reinforced Composites.* ASTM STP 1185 (1994) pp. 278-305

[Sch99] Schulte K.: *Cyclic Mechanical Loading*. Reinforced Plastics Durability: Editor: G.Pritchard, Woodhead Publishing Ltd. Cambridge, UK, (1999) pp.151-185

[Sen81] Sendechkyi G.P.: *Fitting Models to Composite Materials Fatigue Data*. ASTM STP 734, pp. 245-260

[Vas10] Vassilopoulos A.P.: *Fatigue life prediction composites and composites structures*. Elsevier Woodhead Publishing, 576 pages

[VDI2014] VDI 2014: German Guideline, Sheet 3 *Development of Fibre-Reinforced Plastic Components, Analysis*. Beuth Verlag, 2006. (in German and English, author was convenor)

[Wei11] Weinert A. and Gergely P.: *Fatigue Strength Surface: basis for structural analysis under dynamic loads*. CEAS Aeronautical Journal 2011, Vol.2, Issue 1, 243-252

[Wei15] Weißgräber P., Leguillon D. and Becker W.: *A review of Finite Fracture Mechanics: crack initiation at singular and non-singular stress raisers*. Arch. Appl. Mech. DOI 10.1007/s00419-015-1091-7, Springer-Verlag Berlin Heidelberg 2015

# ANNEXES

## AI Cuntze's Failure-Mode-Concept applied to Transversely-isotropic UD Material

### *1 Failure modes and failure assessment*

This chapter is required to define those stress quantities which help to compute the damaging portions. At first, the five well-known fracture failure modes of the transversely-isotropic UD material are shown in *Fig.A1*, see [Cun04]. Presumption: laminas are initially free of essential flaws and are un-notched.
Learnt from observations and inspection results it can be concluded that:

* There are coincidences between brittle UD laminas and brittle isotropic materials
* IFF-Degradation begins with onset of diffuse damaging (hardening) until onset of IFF1 or IFF3

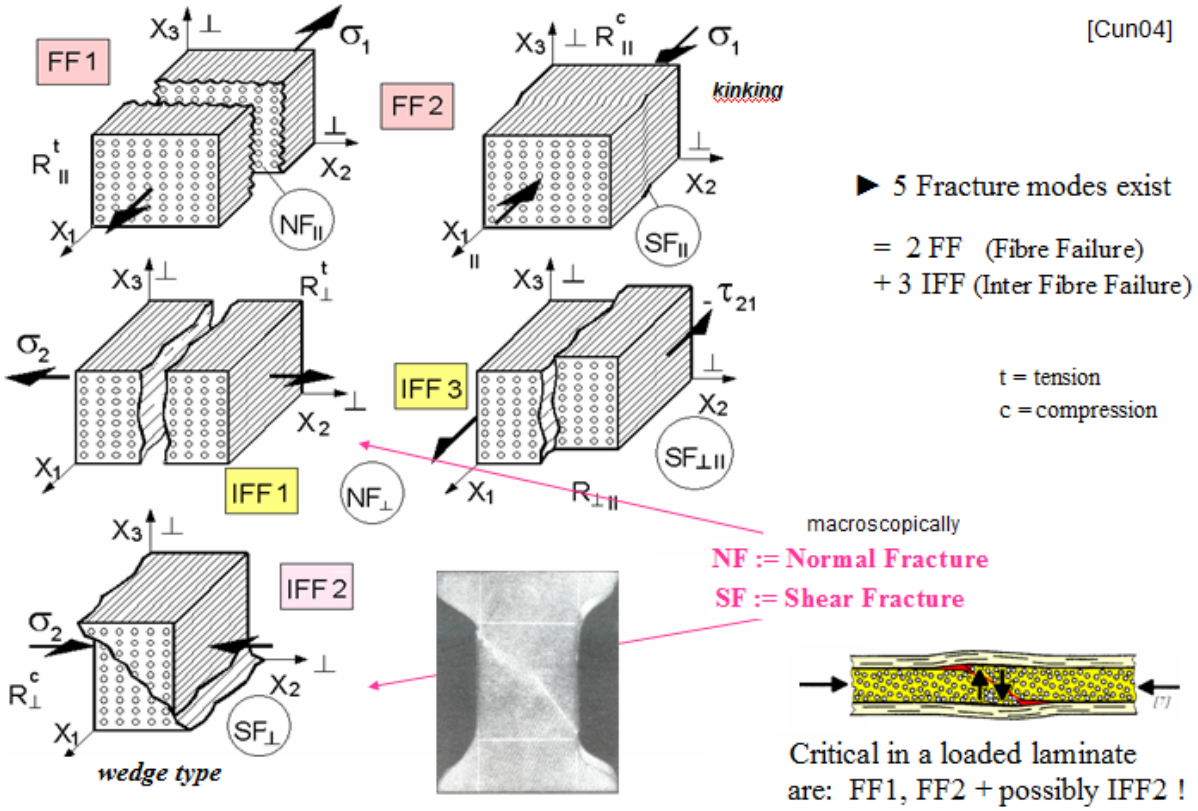


*Fig. A1: Fracture failure modes of UD material, NF = Normal fracture, SF = Shear fracture*

***Definition of Failure:*** structural part does not fulfil its functional requirements such as FF = fiber failure, IFF (= matrix failure), leakage of a vessel, deformation limit, delamination size limit. Design driving failure modes are fixed in each application! Traditionally) are distinguished First-Ply-Failure FPF (nowadays often seen as onset of damaging) and Last-Ply-Failure LPF (final sudden fracture usually after last FF. Failure may be also a distinct degradation as the result of the accumulation of damaging portions.

***Failure Assessment*** includes structure, laminate and lamina (ply, physical layer). Thereby, it is to be discriminated between tolerable and final failure which might be a catastrophic one. Exemplarily for UD material all 5 failure modes Fiber Failure FF1 and FF2, Inter-Fiber-Failure IFF1, IFF2 and IFF3 with their degradation effects must be known, firstly. Onset of failure (First-Ply-Failure) of one ply is predicted by 3D UD strength criteria. Of course, FF means final catastrophic failure. Dependent on the actual case the same may be valid for IFF2,

whereas IFFI (lateral tension) and IFF3 (shear) behave more benign and residual strength and stiffness capacity remain after FPF. The grade of the criticality of a distinct failure needs to be assessed in each project application.

### *2 FMC-based static 3D UD fracture failure conditions and equivalent UD stresses*

*Fig.A2* collects the still mentioned equivalent stresses and material stressing efforts that must be employed in the determination of the damaging portions and the accumulation of them. Added is a typical data range for the friction values $\mu$ of the UD material, the determination of which is presented in [Cun12, 13, Pet16] and its relation to the friction parameter used in the development of the failure conditions. Further, a range for the modes' interaction exponent *m* is presented. The interaction formula represents the static interaction of all mode contributions $Eff^{\text{modes}}$ ,

*Notes: (1) As far as failure mode and failure mechanism remain under cyclic loading, the 'static' formulations above can be transferred from static to cyclic loading! (2) If stability failure can be avoided by straight material test specimens and excellent test rigs then* $R_{||}^{c} \equiv R_{||}^{t}$*, see [Ban16, Sch06]. Only then* $R_{||}^{c}$ *is a real strength entity and not a micro-structural instability result. This is essential for Low Cycle Fatigue LCF.*

### *3 Equivalent stresses and 3D-Failure Surface (failure body)*

***World-Wide-Failure-Exercise***: For transversely-isotropic UD-materials the World-Wide-Failure-Exercises-I and -II have tested the present strength criteria and sorted out the better ones. Cuntze's 3D Failure-Mode-Concept (the 'Mises' under the 3D UD criteria) and Puck's 3D Action Plane-Criteria could map the provided accurate test data best (about 30% of the data sets were not correct or had to be physically interpreted in the WWFE-II). Above 3D strength criteria are also capable of predicting onset-of failure in thickness direction. However, then lower strength values are used in thickness direction than in the lamina plane in order to simply consider the orthotropic material effect on top of the transversely-isotropic lamina material model and analysis. Practice desires macro-mechanical strength failure criteria but – as failure occurs at the constituent level - these criteria must reflect constituents' failures [Cun12]. Failure conditions, combining static strength and fracture mechanics (cracked) are being developed, see [Wei15].

***Limits of a macro-mechanical formulation***: FF cannot be described by a homogenized (smeared) macro-scopical stress $\sigma_1 = \sigma_{\|}$, because filaments do also tensile-break in case of bi-axial compression under a zero external lamina stress loading ($\sigma_1 = 0$) due to the Poisson effect. Hence, the macro-scopical modeling must be replaced by an adequate micro-scopical one. This is formulated engineering-like in macro-scopical quantities by the FEA-delivered macro-mechanical strain ε. Hence, no fiber properties are employed as postulated in Cuntze's Failure Mode Concept.

***Modeling approaches:*** There are several possibilities to model a lamina. The first is to homogenize the constituents matrix and fiber to a lamina material. A second is to stay on the microscopic level of the constituents and bridge by meso-rnodels to the lamina level.
Micro-scopical attempts exist also addressing damaging of the constituent matrix. Here, the macro-scopical approach is preferred.

***Strength Properties:*** Homogenized UD materials have according to their material symmetry (tensorial basis) various strength quantities. These properties are derived by using *isolated* test specimens which show weakest-link behavior (loading of the specimen is terminated when

reaching the strength level IFF). A lamina, embedded in a laminate, experiences a *redundant* behavior and residual capabilities are still available beyond IFF.

***Applicability of Strength Failure Conditions (SFC), Fig A2:*** SFCs are necessary but not sufficient conditions to generally predict strength failure, an energy-based condition (from fracture mechanics) must be used sometimes, too (e.g. when considering the thin-layer effect of laminas embedded in a laminate). A unifying theory from Leguillon, combining strength and fracture mechanics, is found in [Wei15]. In addition to the SCF a fracture mechanics condition is employed and a crack assumed, leading to two equations with two unknowns.

**FF1** $Eff^{\parallel\sigma} = \sigma_1 / \bar{R}^t_{\parallel} = \sigma^{\parallel\sigma}_{eq} / \bar{R}^t_{\parallel}, \qquad \sigma_1 \cong \varepsilon^t_1 \cdot E_{\parallel}$ (matrix negligible). * filament ! modes

**FF2** $Eff^{\parallel\tau} = -\sigma_1 / \bar{R}^c_{\parallel} = +\sigma^{\parallel\tau}_{eq} / \bar{R}^c_{\parallel}, \qquad \sigma_1 \cong \varepsilon^c_1 \cdot E_{\parallel}$

**IFF1** $Eff^{\perp\sigma} = [(\sigma_2 + \sigma_3) + \sqrt{(\sigma_2 - \sigma_3)^2 + 4\tau_{23}^2}\,]/2\bar{R}^t_{\perp} = \sigma^{\perp\sigma}_{eq} / \bar{R}^t_{\perp}$ matrix

**IFF2** $Eff^{\perp\tau} = [(b_{\perp\perp} - 1)\cdot(\sigma_2 + \sigma_3) + b_{\perp\perp}\sqrt{(\sigma_2 - \sigma_3)^2 + 4\tau_{23}^2}\,] / \bar{R}^c_{\perp} = +\sigma^{\perp\tau}_{eq} / \bar{R}^c_{\perp}$ modes

**IFF3** $Eff^{\perp\parallel} = \{[b_{\perp\parallel}\cdot I_{23-5} + (\sqrt{b_{\perp\parallel}^{\,2}\cdot I_{23-5}^{\,2} + 4\cdot \bar{R}_{\perp\parallel}^{\,2}\cdot(\tau_{31}^2 + \tau_{21}^2)^2}\,]/(2\cdot \bar{R}_{\perp\parallel}^{\,3})\}^{0.5} = \sigma^{\perp\parallel}_{eq} / \bar{R}_{\perp\parallel}$

with $I_{23-5} = 2\sigma_2\cdot\tau_{21}^2 + 2\sigma_3\cdot\tau_{31}^2 + 4\tau_{23}\tau_{31}\tau_{21}$

**Modes-Interaction:** ***Eff = 100% = 1***

$$Eff^m = (Eff^{\tau}_{\parallel})^m + (Eff^{\sigma}_{\parallel})^m + (Eff^{\sigma}_{\perp})^m + (Eff^{\tau}_{\perp})^m + (Eff_{\perp\parallel})^m = 1$$

**Typical friction value data range:** $b_{\perp\parallel} = \mu_{\perp\parallel},\ b_{\perp\perp} \cong 1/(1-\mu_{\perp\perp})$

$$0 < \mu_{\perp\parallel} < 0.3,\ 0 < \mu_{\perp\perp} < 0.2,\ 2.5 < m < 3.1$$

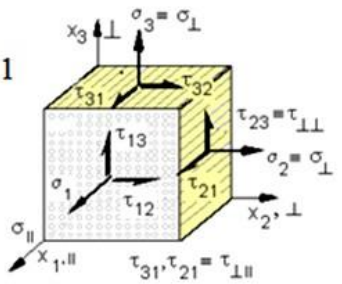


*Fig. A2: FMC-based strength failure conditions (criteria set) [Cun12, 13],* $\sigma_{max} = \sigma_m + \sigma_a$

***Equivalent Stresses***: If one single strength only governs one failure mode, then for the material, equivalent stresses can be defined and formalistically included in a vector for the UD material

$$\left\{\sigma^{mode}_{eq}\right\} = \left(\sigma^{\parallel\sigma}_{eq},\ \sigma^{\parallel\tau}_{eq},\ \sigma^{\perp\sigma}_{eq},\ \sigma^{\perp\tau}_{eq},\ \sigma^{\parallel\perp}_{eq}\right)^T.$$

Herein, the indices σ and τ mark the inherent failure driving stress of the model. The failure surface (failure body), associated to the author's SFCs is depicted in *Fig.A3*. The upper figure belongs to a 2D stress state. When changing the stresses on the coordinates into equivalent stresses $\sigma_{eq}$, then, the same failure surface can be used for the 3D stress state, too.

Matrix failure includes cohesive failure of the shear stress-caused matrix yielding and adhesive failure of the interphase material inclusively diffuse micro-cracking.

***Multi-fold failure mode:*** A stress state $\sigma_2 = \sigma_3$ principally activates the associated failure mode twice. This case is termed a twofold mode (analogous to the isotropic material with the principal stresses $\sigma_I = \sigma_{II}$ or $\sigma_I = \sigma_{II} = \sigma_{III}$ (an hydrostatic threefold NF mode, joint probability). This is of interest for an alternating shear stress $\tau_{21}$ in the Haigh diagram IFF3. *<u>Note</u>: A strength failure condition SFC just describes one failure mechanism wherein all contributing stresses are involved (see e.g. yielding failure by von Mises), In the case of brittle behaving materials the effect of a double occurring failure mode must be considered by an additional part in the formulated SFC.*

***Input for Structural Design*:** In order to achieve a reliable product certification all stochastic design variables like properties and model parameters are required to be statistically based! Generally however, design analysis means investigation of the average behavior of the structural component. Therefore, average (typical) physical properties, including an average stress-strain curve with average values, are applied whereas in design verification of the chosen design statistically-based minimum or maximum properties are utilized. The use of average values results in a structural behavior that meets the real behavior best namely with a 50% expectance value.

*Note: In the case of compression-loaded, brittle behaving materials - according to Mohr-Coulomb - beside strength values also material friction values are mandatory to predict failure!*

***Stress-strain Analysis*:** Analysis shall use project-adequate models to map the structural behavior, selected design-driving Load Cases, cyclic loading spectra, and average physical properties including the stress-strain curve. If a non-linear analysis is necessary then the usually measured hardening curve part (for UD material 3 Inter-Fiber-Failure IFF curves and 2 FFs) as well as the softening curve part after IFF must be provided (after the first FF – due to the usual design – fracture will occur). The softening part of the stress-strain curve represents the decaying stiffness which does not mean zero stiffness. It also represents the remaining strength of the deformation-controlled 'embedded' lamina. This is in contrast to the 'isolated' UD test specimen (material properties determination) with its 'sudden death'.

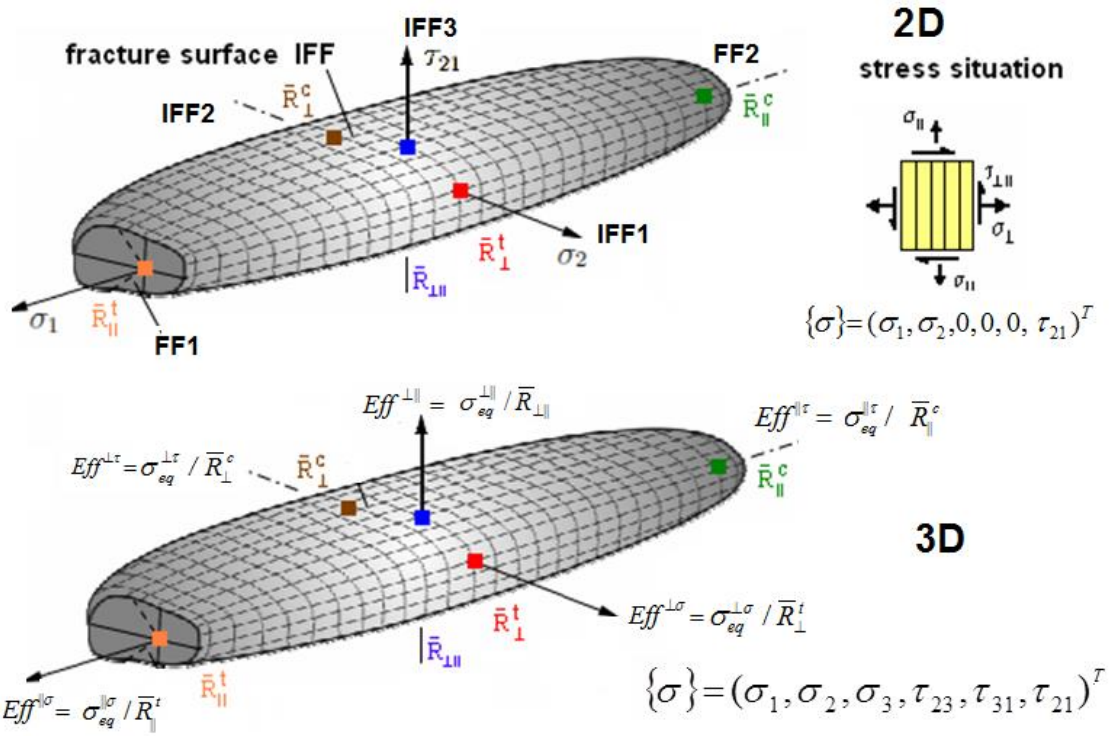


*Fig. A3: 2D and 3D failure surface of the FMC-based strength failure conditions*

*Fig.A4* presents the IFF cross-section of the fracture failure body above. One cross-section belongs to a GFRP UD material the other two to a CFRP UD material. The capability of the interaction formulation is demonstrated in this figure.

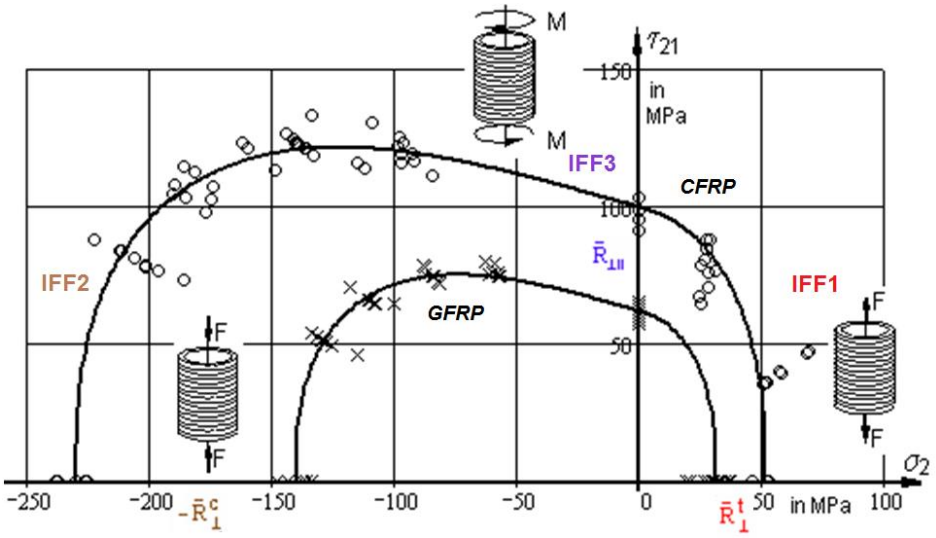


*Fig. A4: IFF cross-section of Fig. A3*

.

***'Isolated' and 'embedded' UD laminas***

As previously mentioned, the designer must differentiate between so-called 'isolated' and 'embedded' laminas. Whereas the isolated test specimens generate strength and hardening curve the embedded test specimens deliver a softening curve, that is of signuficance for non-linear analyses, see *Fig.2* again.

***Global and modal failure conditions** (criteria):*

The following arrangement depicts the difference of a global failure condition (most often used) and a modal failure condition. Global failure conditions are often applied in case of brittle behaving materials, despite of the fact that many modes may become active under operational loading. This means a strong shortcoming [Cun04]. On the other hand, a set of modal failure conditions (SFCs), see below, requires mode-interaction.

*Note: F > = < 1 is termed a failure criterion, so as Christensen correctly does [Chr13] .*

* 1 **global failure condition** : $F(\{\sigma\},\{\bar{R}\}) = 1$ **(usual formulation ! ) ;**

= *'fully interactive conditions' which include several modes*

$\{\bar{R}\} = (\bar{R}_\parallel^t, \bar{R}_\parallel^c, \bar{R}_\perp^t, \bar{R}_\perp^c, \bar{R}_{\perp\parallel})^T$ strength vector

* Set of **mode failure conditions** : $F(\{\sigma\}, R^{mode}) = 1$ **(used in Cuntze's FMC)**

$\{\sigma\} = (\sigma_1, \sigma_2, \sigma_3, \tau_{23}, \tau_{31}, \tau_{21})^T$ vector of stresses

$R^{mode}$ mode-associated strength

The stresses of the stress vector are only partly active in a mode, less than 3 stresses out of 6.

## AII Cuntze's Failure-Mode-Concept applied to Isotropic Material

In order to fully understand the isotropic Haigh diagram – which was used to simpler explain the method - the respective formulas are collected below, wherein $\Theta$ reflects the usual non-circularity of brittle behaving isotropic materials with its different tensile and compressive meridians, see [Cun16, 15a]:

circular: $F^{NF} = \dfrac{\sqrt{4J_2 - I_1^2/3} + I_1}{2 \cdot \bar{R}_t} = 1$ , non-circular: $F^{NF} = \dfrac{\sqrt{4J_2 \cdot \Theta_{NF} - I_1^2/3} + I_1}{2 \cdot \bar{R}_t} = 1$ ,

$$F^{SF} = c_1^{SF} \cdot \frac{3J_2 \cdot \Theta_{SF}}{\bar{R}^{c\,2}} + c_2^{SF} \cdot \frac{I_1}{\bar{R}^c} = 1$$

The invariants used are

$$I_1 = (\sigma_I + \sigma_{II} + \sigma_{III})^T = \; f(\sigma)\;, \quad 6J_2 = (\sigma_I - \sigma_{II})^2 + (\sigma_{II} - \sigma_{III})^2 + (\sigma_{III} - \sigma_I)^2 = \; f(\tau)$$
$$27J_3 = \; (2\sigma_I - \sigma_{II} - \sigma_{III}) \cdot (2\sigma_{II} - \sigma_I - \sigma_{III}) \cdot (2\sigma_{III} - \sigma_I - \sigma_{II})$$

and the non-circularity functions read $\Theta_{NF} = \sqrt[3]{1 + D_{NF} \cdot \sin(3\theta)} = \sqrt[3]{1 + D_{NF} \cdot 1.5 \cdot \sqrt{3} \cdot J_3 \cdot J_2^{-1.5}}$

and $\Theta_{SF} = \sqrt[3]{1 + D_{SF} \cdot \sin(3\theta)} = \sqrt[3]{1 + D_{SF} \cdot 1.5 \cdot \sqrt{3} \cdot J_3 \cdot J_2^{-1.5}}$

with the non-circularity parameters $D_{NF}$ and $D_{SF}$, principally determined from the difference of the tensile and the compressive meridian (is outer than the tensile as the more critical one), see *Fig.A5*. The figure exemplarily displays the obtained fracture failure surface or the fracture body. The material is of a dense consistence.

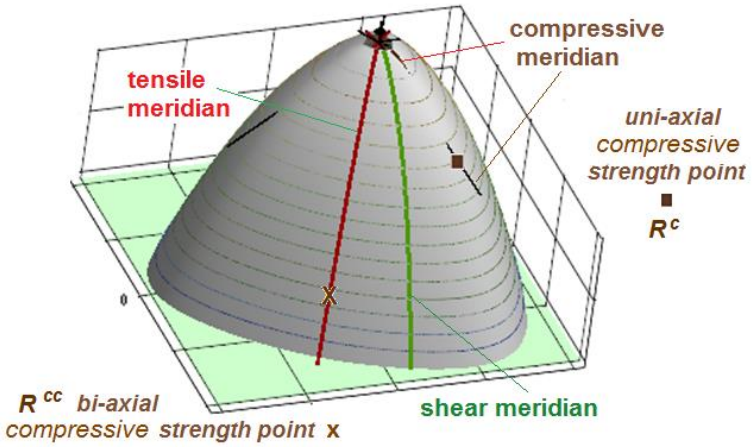


*Fig. A5: Isotropic fracture failure body, displaying the difference of tensile ($\theta$ =+30°, due to the chosen origin = shear meridian) and compressive meridian ($\theta$ =-30°), $D_{NF}$=0.79, $D_{SF}$=15, $\theta_{fpc}$=50°, m=2.6*

*Note: Non-circularity is linked to the so-called 360°/3 = 120°-symmetry of isotropic materials where the three principal stresses are equal and can be exchanged with no restriction.*

The curve parameters follow from test data evaluation (fitting procedure) or determination of

$$c_2^{NF} = (-3 \cdot \theta_{fpc} + 1)/(3 \cdot \theta_{fpc} + 1) = (1 + 3 \cdot \mu)/(1 - 3 \cdot \mu), \quad c_1^{SF} = 1 + c_2^{SF}.$$
$$\mu \;=\; \cos\,(2 \cdot \theta_{fpc}° \cdot \pi / 180\;).$$

Thereby, the friction value $\mu$ can be determined by measuring the fracture plane angle $\theta_{fpc}$ under compressive fracture. With respect to the difficult mearurement of the fracture angle another approach has been performed in [Pet16].

From the failure functions the following material stressing efforts are derived:

$$Eff^{NF} = c_{NF} \cdot \frac{\sqrt{4J_2 \cdot \Theta_{NF} - I_1^2/3} + I_1}{2 \cdot \overline{R}_t} = \; \sigma_{eq}^{NF} / \overline{R}_t \;,$$

$$Eff^{SF} = \frac{c_2^{SF} \cdot I_1 + \sqrt{(c_2^{SF} \cdot I_1)^2 + 12 \cdot (c_1^{SF} \cdot 3J_2 \cdot \Theta_\tau)}}{2 \cdot \overline{R}^c} = \; 1.$$

Mode-interaction is considered - analogous to the transversely-isotropic material - by

$$Eff \;\; = [(Eff^{NF})^m + (Eff^{SF})^m]^{m^{-1}} \;=\; 100\% \;.$$

*Note for further explanation: ductile, $\mu$ = 0, yield planes under* 45°; *brittle, $\mu$* = 0.17, $\theta_{fpc}$ 50° or $\mu$ = 0.31, $\theta_{fpc}$=55°. *Recommended is* $0.1 < \mu < 0.2$ *(smaller value is conservative).*

## B Visualisation of the Calculation of a Damaging Portion with Lifetime Prediction

*Fig.A6* displays the author's procedure of a UD lifetime prediction for High Cycle Fatigue.

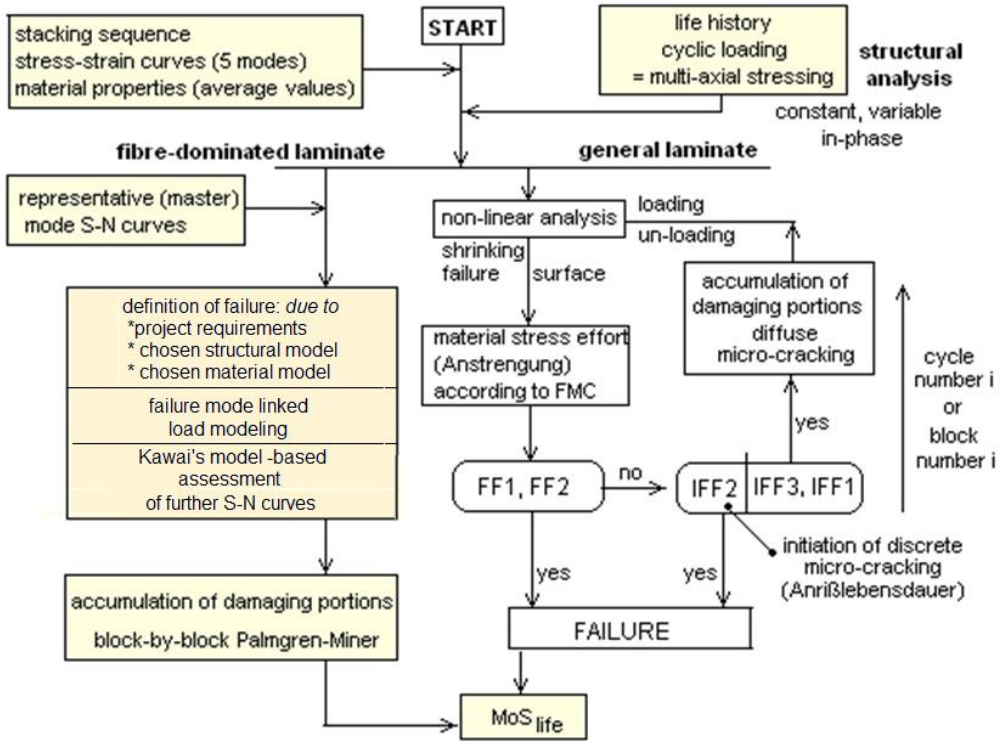


*Fig. A6: FMC-based UD lifetime prediction for HCF*

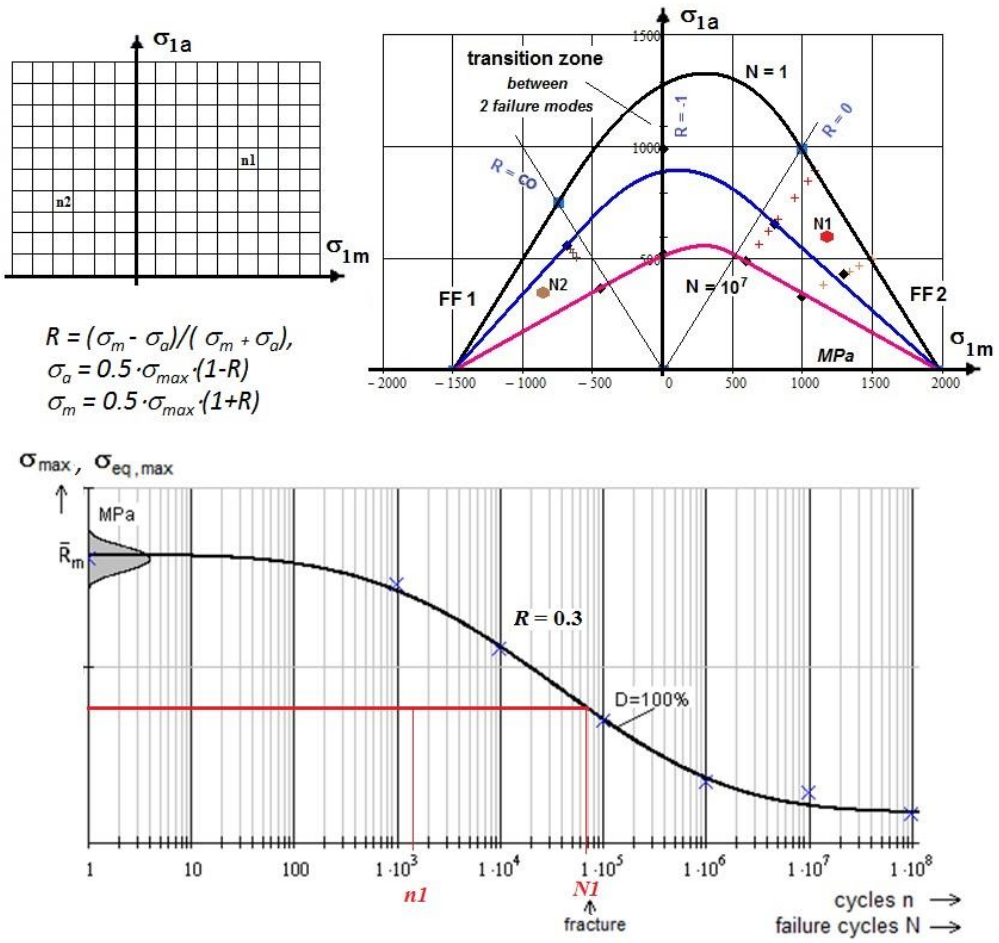


*Fig. A7: FF-linked example for the determination of a damaging portion, FF1*

*Fig A8* presents an FF –linked example for the determination of damaging portions. There are two stress states indicated in the Haigh Diagram. Exemplarily, just for $n_1$ the necessary S-N curve in Fig.A7 was provided.
For the first of the two marked loading cycles $n(\sigma_{1a},\sigma_{1m})$ the calculation delivers $D_{\|1} = n_1/N_1$ (FF1 mode) and for the second $D_{\|2} = n_2/N_2$ (FF2 mode).

The popular *rain-flow counting method* (from T. Endo and M. Matsuishi, 1968) is used in order to reduce a spectrum of varying stresses into a set of simple stress reversals. Its importance is that it allows the application of Miner's rule in order to estimate the fatigue life under complex loading.

## C Notations for Strength Properties

In order to clearly denote strength and avoid misinterpretations the author put – on basis of the performed VDI 2014–investigations – the table below together. The internationally applied notations have been considered, see also [Cun16c].

*Table A1:Self-explaining symbolic notations for strength properties (proposed for ESA, 2007)*

| | Fracture **Strength Properties** | | | | | | | | | |
|---|---|---|---|---|---|---|---|---|---|---|
| | **loading** | **tension** | | | **compression** | | | **shear** | | | |
| | **direction** or **plane** | 1 | 2 | 3 | 1 | 2 | 3 | 12 | 23 | 13 | |
| **9** | **general orthotropic** | $R_1^t$ | $R_2^t$ | $R_3^t$ | $R_1^c$ | $R_2^c$ | $R_3^c$ | $R_{12}$ | $R_{23}$ | $R_{13}$ | **Friction propert.** |
| **5** | **UD** | $R_{\|\|}^{\ t}$ NF | $R_{\perp}^{\ t}$ NF | $R_{\perp}^{\ t}$ NF | $R_{\|\|}^{\ c}$ SF | $R_{\perp}^{\ c}$ SF | $R_{\perp}^{\ c}$ SF | $R_{\|\perp}$ SF | $R_{\perp\perp}$ NF | $R_{\|\perp}$ SF | $\mu_{\perp\perp}$, $\mu_{\perp\|}$, |
| **6** | **fabrics** | $R_W^t$ | $R_F^t$ | $R_3^t$ | $R_W^c$ | $R_F^c$ | $R_3^c$ | $R_{WF}$ | $R_{F3}$ | $R_{W3}$ | *Warp = Fill* |
| **9** | **fabrics general** | $R_W^t$ | $R_F^t$ | $R_3^t$ | $R_W^c$ | $R_F^c$ | $R_3^c$ | $R_{WF}$ | $R_{F3}$ | $R_{W3}$ | $\mu_{W3}$, $\mu_{F3}$, $\mu_{WF}$ |
| **5** | **mat** | $R_{1M}^t$ | $R_{1M}^t$ | $R_{3M}^t$ | $R_M^c$ | $R_{1M}^c$ | $R_{3M}^c$ | $R_M^\tau$ | $R_M^\tau$ | $R_M^\tau$ | *(UD, turned direction)* |
| **2** | **isotropic matrix** | $R_m$ SF | $R_m$ SF | $R_m$ SF | *deformation-limited* | | | $R_M^\tau$ | $R_M^\tau$ | $R_M^\tau$ | $\mu$ |
| | | $R_m$ NF | $R_m$ NF | $R_m$ NF | $R_m^c$ SF | $R_m^c$ SF | $R_m^c$ SF | $R_m^\sigma$ NF | $R_m^\sigma$ NF | $R_m^\sigma$ NF | $\mu$ |

*NOTE: *As a consequence to isotropic materials (European standardisation) the letter R has to be used for strength. US notations for UD material with letters X (direction 1) and Y (direction 2) confuse with the structure axes' descriptions X and Y . *Effect of curing-based residual stresses and environment dependent on hygro-thermal stresses. *Effect of the difference of stress-strain curves of e.g. the usually isolated UD test specimen and the embedded (redundancy ) UD laminae. $R_m$ := 'resistance maximale' (French) = tensile fracture strength (superscript t here usually skipped), R:= basic strength. Composites are most often brittle and dense, not porous! SF = shear fracture*